Litter quality outweighs climate as a driver of decomposition across the tundra biome

Thomas, Haydn J. D.[1]; Myers-Smith, Isla H.[1]; Høye, Toke T.[2]; Petit Bon, Matteo[3,4].; Lembrechts, Jonas[5]; Walker, Eleanor R.[1]; Björnsdóttir, Katrín[6,7]; Barrio, Isabel C.[8]; Jónsdóttir, Inga Svala[6]; Venn, Susanna[9]; Alatalo, Juha M.[10]; Baltzer, Jennifer L.[11], Wallace, Cory A.[11]; Ackerman, Daniel E.[12]; Gough, Laura[13]; Prevéy, Janet S.[14,15]; Rixen, Christian[15]; Carbognani, Michele[16]; Petraglia, Alessandro[16]; Christiansen, Casper T.[17]; Inouye, David W.[18,19]; Ogilvie, Jane E.[19]; Trouillier, Mario[20]; Wilmking, Martin[20]; Treharne, Rachel[21]; Angers-Blondin, Sandra[1]; Urbanowicz, Christine[22]; von Oppen, Jonathan[2,15]; Wipf, Sonja[15]; Smith, Paul A.[23]; Suzuki, Satoshi N.[24]; Suzuki, Ryo O.[25].; Virkkala, Anna-Maria[26]; Luoto, Miska[26]; Serikova, Svetlana[27]; Bjorkman, Anne D.[7,28]; Blok, Daan[29]; Gallois, Elise C.[1]; Sarneel, Judith M.[27]

1. School of Geosciences, University of Edinburgh, UK
2. Aarhus University, Denmark
3. University Centre in Svalbard, Svalbard
4. Arctic University of Norway, Norway
5. University of Antwerp, Belgium
6. University of Iceland, Iceland
7. University of Gothenburg, Sweden
8. Agricultural University of Iceland, Iceland
9. Deakin University, Australia
10. Qatar University, Qatar
11. Wilfrid Laurier University, Canada
12. University of Minnesota, USA
13. Towson University, USA
14. USDA Forest Service Pacific Northwest Research Station, Washington, USA
15. WSL Institute for Snow and Avalanche Research SLF, Switzerland
16. University of Parma, Italy
17. Bjerknes Centre for Climate Research, Norway, Norway
18. University of Maryland, USA
19. Rocky Mountain Biological Laboratory, Colorado, USA
20. University of Greifswald, Germany
21. University of Sheffield, UK
22. Dartmouth College, New Hampshire, USA
23. Environment and Climate Change Canada, Canada
24. University of Tokyo, Japan
25. University of the Ryukyus, Japan
26. University of Helsinki, Finland
27. Umeå University, Sweden

28. Senckenberg Gesellschaft für Naturforschung, Biodiversity and Climate Research Centre (BiK-F), Germany
29. Lund University, Sweden

Author contributions: HT and IMS conceived the study, IMS supervised the research. JS devised and helped to adapt the Tea Bag Index for tundra settings. Data were collected by all authors except AB, DB and JS. HT compiled the tundra teabag dataset. HT and AB performed statistical analysis. HT wrote the manuscript with input from IMS, AB, EG, JvO, KB and contributions from all authors.

Acknowledgements:

The project was funded by the UK Natural Environment Research Council (ShrubTundra Project NE/M016323/1 & PhD Studentship NE/L002558/1 [HT]), The Swedish Research Council (Grant/Award Number: 2015-00465), Marie Skłodowska Curie Actions (Grant/Award Number: INCA 600398), The University of Iceland Research Fund, Polar Knowledge Canada, ArcticNet, NSERC Changing Cold Regions Network, Research Foundation Flanders (FWO), the International Network for Terrestrial Research and Monitoring in the Arctic (INTERACT), the Swedish Research Council (VR), the Strategic theme Sustainability of Utrecht University (sub-theme Water, Climate and Ecosystems), Carl Tryggers stiftelse för vetenskaplig forskning, Qatar Petroleum, US National Science Foundation (Grant 1637459), German Research Council (DFG GraKo 2010 Response), the Svalbard Environmental Protection Fund (Project grant 18/00517-3), the Norwegian Research Council (Project grant 269957/E10), Carlsberg Foundation Grant (CF14-0992), the Academy of Finland (project number 286950), the Otto A. Malm foundation, Societas pro Fauna et Flora Fennica and Nordenskiöld-samfundet. Additional data and contributions were the Government of the Northwest Territories - Laurier Partnership, Philip Marsh, Marlene Doyle, Kouichi Takahashi, Hajime Kobayashi, Mitsuru Hirota, Hideyuki Ida, Yasuo Iimura, Tatsuyuki Seino, billy barr, Annika Kristoffersson, Marc-André Lemay, Gergana Daskalova, Nadine Gilmour, the staff and research commission of the Swiss National Park, BioGeoClimate Modelling Lab. We thank the innumerable field technicians, logistics teams, graduate and undergraduate assistants for help with data collection. Special thanks to the Tea Bag Index core-team. Finally, we thank parks, wildlife refuges, field stations and the local and Indigenous people for the opportunity to conduct research on their land.

Abstract

Considerable uncertainty exists regarding the strength, direction and relative importance of the drivers of decomposition in the tundra biome, partly due to a lack of coordinated decomposition field studies in this remote environment. Here, we analysed 3717 incubations of two uniform litter types, green and rooibos tea, buried at 330 circum-Arctic and alpine sites to quantify the effects of temperature, moisture and litter quality on decomposition. We found a surprisingly linear positive relationship between decomposition and soil temperature across all sites, counter to theory and previous model estimates. Litter mass loss was greater at wetter sites, even where soils reached almost full water saturation. However, litter quality was the strongest driver of litter mass loss across the tundra biome, explaining six times more variation in summer decomposition than soil temperature. Our results indicate that climate warming will directly increase decomposition across tundra environments. However, the indirect effects of climate change on vegetation communities, and thus plant litter inputs and quality, could have a more profound impact than direct effects on the balance of this globally important carbon store.

Introduction

The decomposition of terrestrial carbon pools is a vital component of the global carbon cycle[1,2] and is sensitive to temperature[3]. Climate warming is predicted to accelerate both the decomposition process and carbon emissions[2,4,5]. Quantifying changes in decomposition is thus critical for identifying major feedbacks to climate change[6]. Perhaps nowhere is this more true than in high-latitude ecosystems, which contain over a third of global soil carbon[7,8], more than double the current atmospheric stocks[9]. Decomposition in the tundra is currently constrained by cold temperatures, frozen soils and recalcitrant litter, encouraging the build-up of organic matter in soils[10]. Tundra ecosystems are warming at up to four times the global average rate[11], with annual temperatures in the Arctic predicted to increase by 2-10°C by the end of the century relative to the period from 1850 to 1900[12]. As a result, decomposition rates are expected to increase in the tundra [10], potentially releasing 37 to 174 Pg of carbon by 2100, equivalent to an additional 17 to 82 ppm CO_2 in the Earth's atmosphere[13]. Climate warming impacts can either directly reduce carbon stores by accelerating decomposition [10], or indirectly by changing plant litter inputs[14,15]. In addition, warming impacts on decomposition are not occurring in isolation from other environmental change including changes to soil moisture[16,17]. Arctic carbon emissions could determine whether soils globally are a sink or source of carbon under accelerating global change[6]. Thus, there is an urgent need to explore the drivers of decomposition across the tundra biome.

Despite the potential substantial impact of climate change on carbon cycling in Arctic terrestrial ecosystems, the relative influence of environmental drivers of decomposition have yet to be experimentally tested at the tundra biome scale. Temperature and soil moisture are considered to be the primary drivers of decomposition[10], and together explain approximately 70% of variation in decomposition rates globally[2,18,19]. However, biogeochemical models incorporate substantially different relationships between decomposition, temperature and soil moisture, particularly at climatic extremes[20] (Fig. 1). Earth system model relationships between temperature and decomposition rate are either assumed to exponentially decline or saturate near zero at sites with colder temperatures and relationships with moisture vary between saturating, optimal, linear or sigmoidal relationships[21] (Fig. 1). This lack of consistency in the assumed relationships between both soil temperature and moisture and decomposition is partly driven by a lack of real-world data from high-latitude regions[5,21], and contributes to the large uncertainty surrounding predictions of global soil carbon losses[4,5]. Thus, reducing this uncertainty requires *in situ* decomposition data across a range of temperature and moisture conditions within the tundra biome.

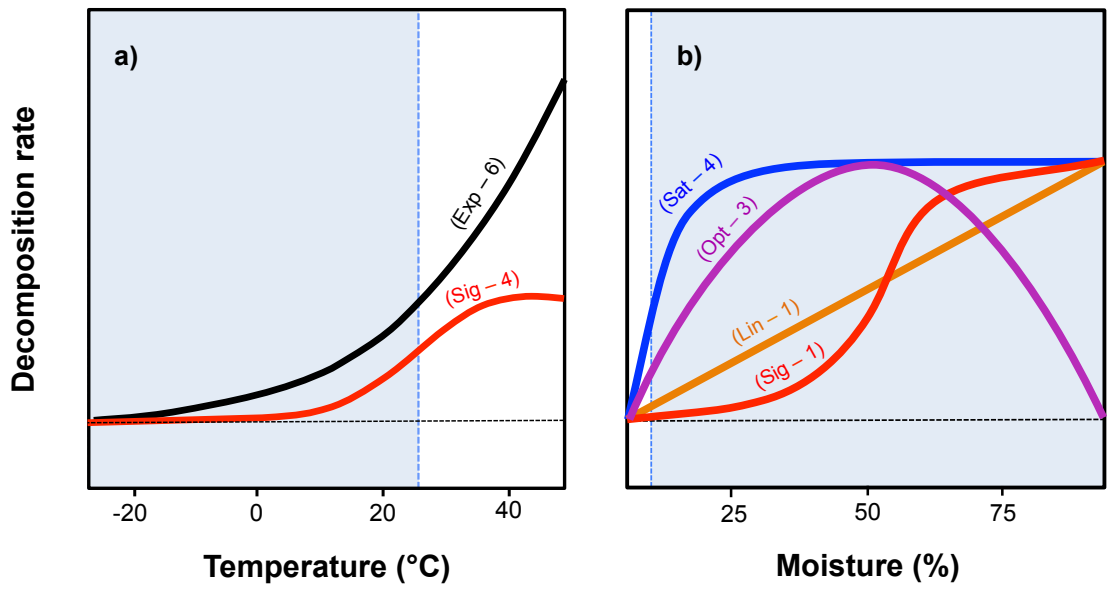

Figure 1. Biogeochemical models include a number of different shapes of relationships between decomposition rate of soil organic matter and temperature (a) and moisture (b). Summary of 19 biogeochemical model functions included in Sierra et al. 2015. The relationship between decomposition and temperature is modelled as exponential (Exp: black, six models) or sigmoidal (Sig: red, four models). The relationship between decomposition and moisture is modelled as saturating (Sat: blue, four models), optimal (Opt: purple, three models), linear (Lin: orange, one model) or sigmoidal (Sig: red, one model). The blue shaded area indicates the range of temperatures and soil moisture values for the 330 sites included

in this study. Note that temperature conditions generally do not exceed ~25°C in the tundra biome.

Soil organic matter has many forms, one of which is leaf litter deposited on the soil surface and incorporated into the soil profile over time including through cryoturbation processes in tundra ecosystems[22]. Decomposition of leaf litter is dependent on litter quality, and thus the structural and chemical traits of plant tissues of different species across ecological communities[23–27]. Plant traits and litter characteristics may be the dominant control on litter decomposition worldwide, outweighing environmental drivers even across biomes[24,28,29]. As plant community composition changes with warming, so too will the litter inputs to the soil and decomposition rates of soil organic matter[14]. Many tundra plant communities are undergoing widespread changes[30], notably an expansion of shrub species[31,32], that could dramatically alter litter inputs to soils[15]. Site-scale experiments indicate that litter quality explains more variation in litter decomposition than environmental variables[25,33,34]. Cross-site studies of decomposition using common substrates have been conducted for other global biomes[19,21,24,28,29,35–37]. However, the relative influence of litter quality versus environmental controls on decomposition has not yet been tested across the tundra biome, primarily due to difficulties of controlling for litter homogeneity.

In this study, we quantify the drivers of litter decomposition at 330 sites across the circum-Arctic and alpine tundra (Table S1) and 3717 incubations using the Tea Bag Index[18]. The Tea Bag Index is a standardised protocol that employs two commercially available types of tea (labile green and recalcitrant rooibos tea) to estimate stabilisation factor (S) and decomposition rate (k) and provide a highly replicable method for measuring leaf litter decomposition across sites[18,28,38]. Decomposability of the two tea types is also representative of leaf litters for a range of tundra species (Fig. 2) and thus provides an analogue for the potential impact of plant community change on litter decomposability in tundra ecosystems[14,27,39–41]. Due to relationships described in theoretical and experimental studies[2,20,21,25], we predict that decomposition will increase exponentially with temperature, and that temperature will be the strongest driver of decomposition across the broad biogeographical gradients of the tundra biome.

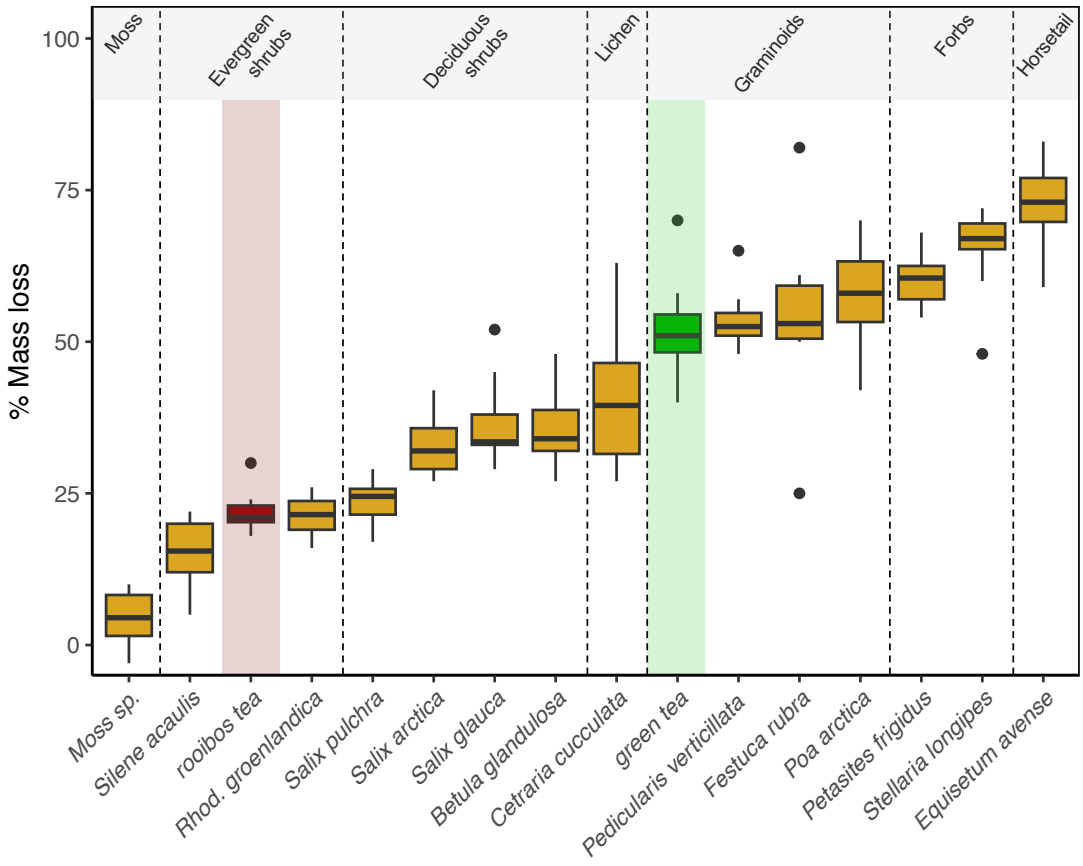

Figure 2. Annual mass loss of green and rooibos tea compared to mass loss of a range of representative tundra species. Tea types are indicated by red (rooibos tea) and green (green tea) boxplots. Tundra species were collected from two sites: the Kluane Range Mountains, Yukon, Canada (62°N) and Qikiqtaruk-Herschel Island, Yukon, Canada (70°N). All litter and tea were decomposed for one year in a common litter bed at 5-8cm depth at Kluane Lake following methods outlined in Cornelissen et al. (2007), with 10 replicates per species' litterbag and tea type.

Results

We found that summer mass loss increased linearly with soil temperature (Fig. 3b) across tundra sites by 1.94% ± 0.31% per °C for labile green tea and 1.09% ± 0.29% per °C for recalcitrant rooibos tea. Relationships were consistent across incubation periods (Figs. S1-S2) and decomposition metrics (Figs. S3-S4), with higher temperatures associated with a lower stabilisation factor (*S*) and a faster decomposition rate (*k*). Within-site mass loss also increased with soil temperature (Fig. S5).

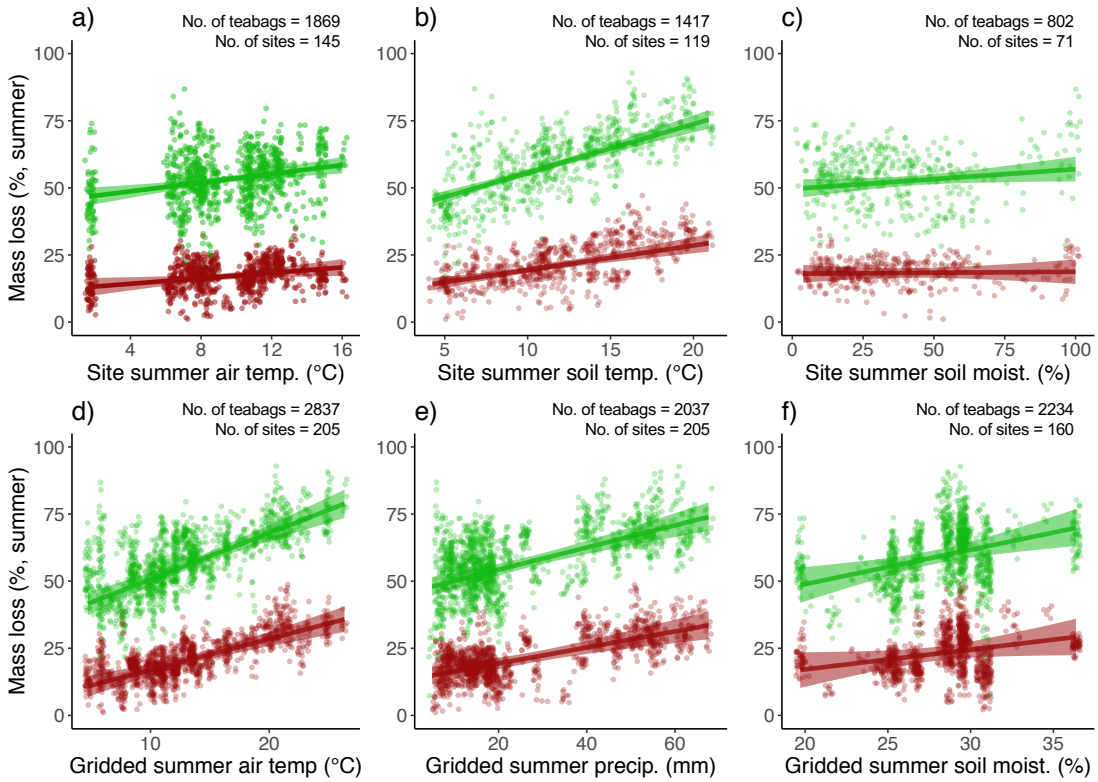

Figure 3. Relationships between litter decomposition, climate and environmental variables were linear across the range of environmental conditions found across study sites (see also Fig. S6 for non-linear models). Plotted relationships are between litter decomposition (mass loss), locally-measured environmental variables (a-c) and gridded climate data (d-f) for the summer incubation period (see also Fig. S1 for winter incubations and Fig. S2 for year-long incubations). Points indicate individual tea bag replicates across all sites. Lines indicate hierarchical Bayesian model fit with 97.5% credible intervals. Colours indicate tea type (red = rooibos tea, green = green tea). See Table S2 for model outputs.

Summer mass loss increased with locally-measured soil moisture across tundra sites (green tea: 0.07% ± 0.06% per % moisture, rooibos tea 0.01% ± 0.06% per % moisture, Fig. 3c), and notably did not decrease at high moisture values, even where soils reached saturation such as on Svalbard (Figs. 3 and S6).

Relationships for winter and year-long incubations were weaker than for summer incubations (Figs. S1-2). Mass loss showed a weak positive relationship with soil moisture within sites (Fig. S5). Soil moisture did not influence the relationships between soil temperature and mass loss, but litter mass loss was higher at wetter versus drier sites at any given temperature (Fig. S7).

Relationships across sites were best explained by linear, rather than exponential, relationships for temperatures. For soil moisture in the Western Hemisphere of the Arctic, relationships across sites were best explained by a linear relationship and for the Eastern Hemisphere, an exponential relationship driven by high mass loss at soil moisture values above 75% volumetric water content experienced at sites in Svalbard (Fig. S6).

Litter quality was the strongest predictor of litter decomposition (Fig. 4a-c), explaining six and ten times more variation in summer mass loss than soil temperature and soil moisture, respectively. This strong effect of litter quality was maintained across incubation periods (Fig. 4d-f) and mass loss of the two tea types did not converge after two years (Fig. S8).

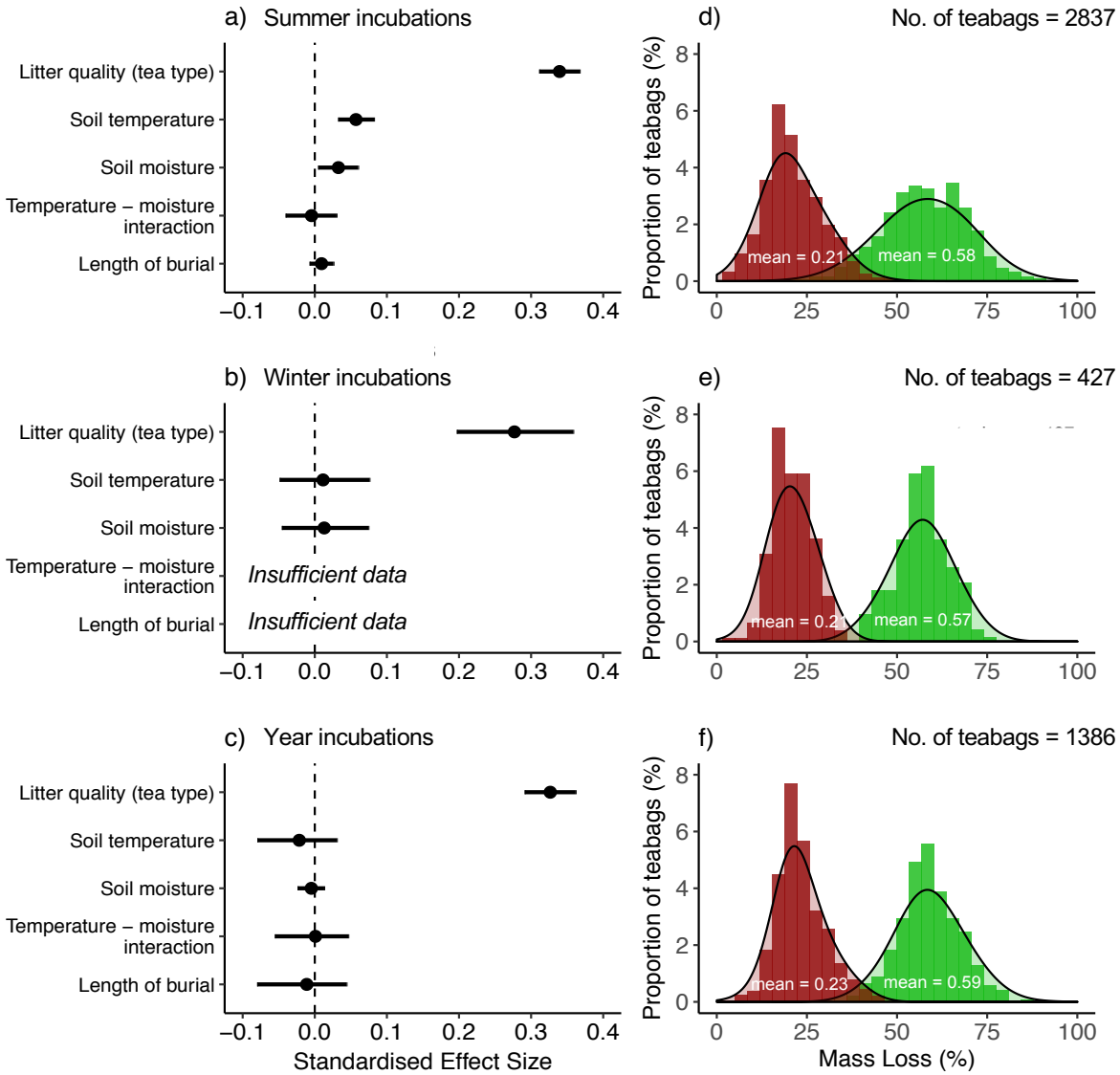

Figure 4. Litter quality explained greater variation in litter decomposition than environmental variables. Standardised effect sizes of locally-measured environmental variables and litter

substrate for summer incubations, winter incubations and year incubations (a-c). We did not have enough variation in incubation period to calculate the effect of length of burial (days within each incubation period) and the dataset was not large enough to test for a temperature-moisture interaction for winter incubations. Distribution of mass loss values for the two litter substrates (rooibos tea – red, green tea – green) for summer, winter and year incubations (d-f).

Relationships using gridded climate data were consistent with site-level climate data (Figs. 3, S1 and S2). We found strong relationships between decomposition and all gridded climate variables (Fig. 3d-f) and the interaction between gridded temperature and moisture similarly suggested greater mass loss in wetter sites (Fig. S7). Extrapolating relationships across tundra and subarctic regions based on gridded climate and soil moisture revealed strong spatial variation in decomposition along biogeographic gradients (Fig. 5).

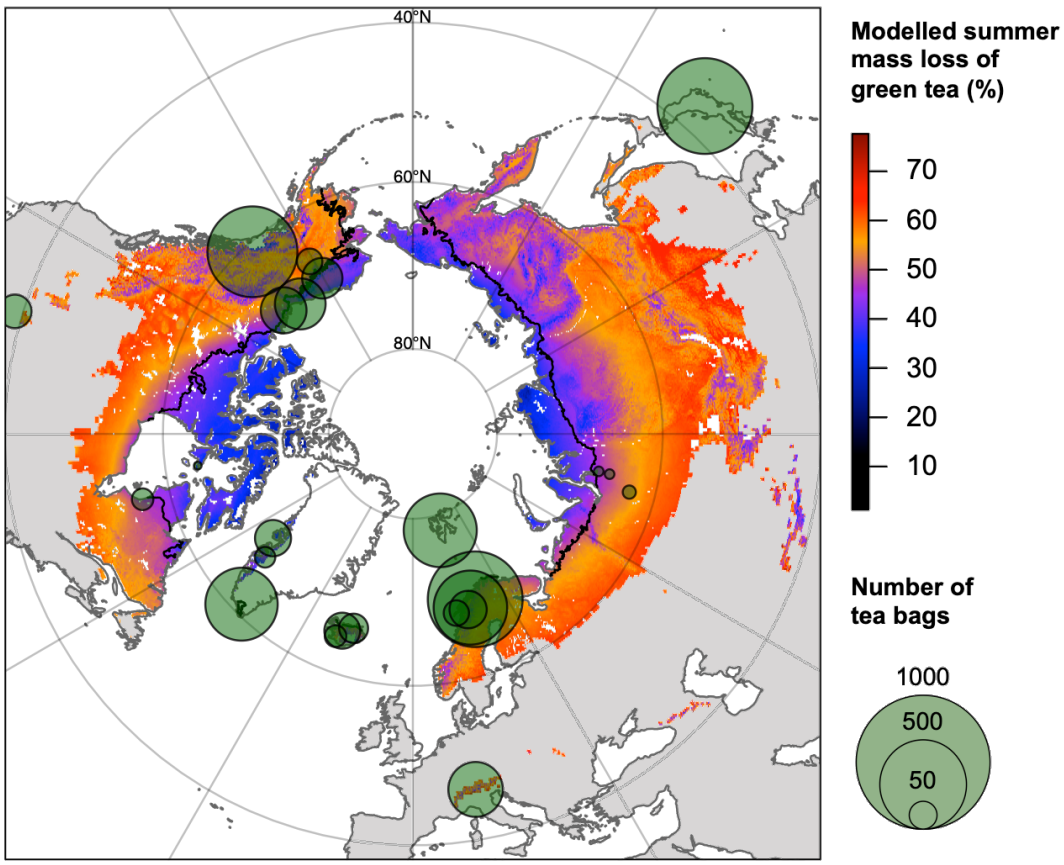

Figure 5. Modelled summer decomposition (percent mass loss) of green tea for tundra and sub-Arctic regions based on 1979 to 2013 mean summer air temperature (Climatologies at high resolution for the Earth's land surface, CHELSA) and soil moisture (European Space Agency data, ESA) from 1979 to 2013. Field collection locations are illustrated by green

239 circles, grouped by geographic region (Table S1, figure excludes Australian alpine region).
240 Circle size indicates the number of tea bag replicates within each geographic region. Tundra
241 and sub-Arctic classifications are based on Köppen-Geiger classification[42]. Ice-covered areas
242 are excluded. The circum-Arctic treeline is indicated with a black line[43].
243
244 **Discussion**
245 Contrasting with theory and model estimates, we find strong linear relationships, rather than
246 exponential, between decomposition and soil temperature and moisture across the tundra
247 biome (Fig. 3). Our findings provide comprehensive evidence that climate-driven changes to
248 plant communities, and thus litter quality, could have a greater impact on litter decomposition
249 than the direct effects of warming in the tundra (Fig. 4). Our results align with site-specific
250 studies that find that decomposition is more strongly influenced by litter quality than climatic
251 variability[14,25–28,33,34,41]. Many sites across the tundra are currently undergoing rapid vegetation
252 change[30,44,45], notably an increase in shrub species with relatively recalcitrant litter, which in
253 many cases are out-competing graminoids with relatively labile litter[31,32]. This vegetation
254 change has been hypothesised to partly counteract the effects of warming on litter
255 decomposition[15]. Our results suggest that the biotic effects of vegetation change could
256 outweigh the direct effects of warming on tundra litter decomposition, though biotic changes
257 will likely occur more slowly and lag behind warming[14,44].
258
259 We found positive linear relationships between decomposition, soil temperature and soil
260 moisture, with the greatest decomposition occurring in warmer and wetter sites (Fig. 3, Fig.
261 S7). Our 330 study sites encompass the linear range of global biogeochemical modelled
262 relationships of temperature and decomposition, but the non-linear range of soil moisture (Fig.
263 1, [20]). Thus, our findings indicate that soil moisture may play a key role in mediating the effects
264 of warming on litter decomposition across the temperature-limited tundra biome. Based on
265 these relationships, we estimate that predicted Arctic warming of 2 to 10°C over the 21st
266 century could double summer litter mass loss at the coldest tundra sites. However, changes
267 are highly contingent upon site-specific factors, including moisture availability, substrate
268 quality and decomposer community[14,23,24,26–29,39,46,47]. Although we focus on short-term
269 decomposition processes, greater early-stage decomposition could accelerate
270 biogeochemical cycling[48] and stimulate the loss of older organic carbon[15,49] through nitrogen
271 mining[50–52] or priming of microbial communities[22,53,54].
272
273 Contrary to the relationships assumed in many Earth system models[20], we observed neither
274 an exponential increase in decomposition with temperature[19], nor a decrease in
275 decomposition at the highest moisture values (Fig. 3). However, we observed considerable

276 within-site variation in decomposition, emphasising the importance of site-specific factors[46]
277 such as microbial community[55] and soil chemistry[56]. We explored the site-level relationships
278 with general additive models, and found that overall relationships between environmental
279 variables and decomposition were best fit by linear relationships across variation in
280 temperature and soil moisture (Fig. S6). However, we did find that for the Eastern Hemisphere,
281 there was an exponential relationship between mass loss and soil moisture driven by data
282 from Svalbard (Fig. S6). Overall, our findings could indicate that decomposition is
283 underestimated at colder or wetter tundra sites, but overestimated at warmer sites in current
284 model simulations.
285
286 Discrepancy between field observations and modelled decomposition could be caused by
287 environmental interactions. Environmental drivers such as warming and freeze-thaw
288 dynamics may have different influences across the year [33]. With warming, higher temperatures
289 dry surface soils and reduce decomposer activity[57], as has been observed in warming
290 experiments[16,58] and long-term monitoring[59]. Biotic changes to either plant[14,26,28] or
291 decomposer communities[51,60,61] may also respond in complex ways to environmental change.
292 In addition, spatial patterning of landforms and environmental change such as permafrost thaw
293 can create wetter and drier microclimates within the same landscapes that can alter
294 decomposition across scales[39,41,62]. Accounting for real-world biotic and abiotic patterns and
295 interactions among the drivers of decomposition in Earth system models will be critical to more
296 accurately projecting the effects of warming on decomposition and resulting losses to carbon
297 stores[17,19,20,57].
298
299 Our tundra-wide decomposition experiment has a number of caveats. Green and rooibos tea
300 are not tundra plant species, but they do encompass the decomposability of tundra plant
301 species (Fig. 2) and thus provide an excellent common substrate for decomposition studies.
302 Although tea undergoes leaching processes, losing mass due to the loss of water-soluble
303 compounds during *in situ* decomposition[63], so too do tundra plants[38]. We tested leaching rates
304 in our study, finding ~20% greater mass loss for green tea and ~7% greater mass loss for
305 rooibos tea in two-month incubations rather than in 24-hour incubations in liquid water. We
306 found no substantial difference in mass loss with replacement of water across incubations
307 (Fig. S9), suggesting that leaching processes with lateral water flow is likely not a major driver
308 of mass loss in Tea Bag Index studies. Our study only encompasses short-term decomposition
309 with incubation lengths from three months to two years. Litter quality may have a weaker effect
310 on decomposition over longer time periods, and climate or other environmental influences may
311 become stronger over time[64–67]. We used gridded climate data for our tundra-wide
312 extrapolation and for climate data at sites where *in situ* measurements were not recorded.

Gridded climate data at high latitudes are extrapolated from more limited meteorological data than at lower latitudes, and at high latitudes, precipitation data are particularly limited[68]. Thus, extrapolations of our statistical results across the tundra biome contain substantial inherent uncertainty (Fig. 5). However, our results suggest that decomposition can indeed be mapped across large scales[69], serving as a useful tool for predicting future decomposition.

Changing decomposition rates will have profound implications for the global carbon cycle as the climate is warming [2]. Warming-induced acceleration of litter decomposition could greatly increase carbon losses in the tundra and other high-latitude ecosystems[6], which have historically acted as long-term carbon sinks[13,70]. Tundra regions are also predicted to undergo some of the greatest carbon losses over the coming century[4], although predictions are highly sensitive to data availability[5]. Our study provides well-resolved statistical relationships from standardised field observations that can be used to parameterise Earth system models and refine estimates of this critical feedback to the global carbon cycle. Ultimately, our findings indicate that climate change is likely to increase decomposition across the tundra biome, but that warming-induced vegetation change could have even more pronounced repercussions for this globally important high-latitude carbon store.

Methods

We buried 5647 tea bags *in situ* at 5-8 cm depth at 330 sites across the tundra biome (Fig. 2, Table S1). Our database has a hierarchical structure with plots (geographic areas including multiple tea bag incubations) within sites (unique grid referenced locations of multiple plots) within grid cells (the pixels of the gridded climate data, Table S1).

We recovered tea after three- (summer), nine- (winter), twelve-month (year) and two-year incubations and calculated three metrics of decomposition: (1) percent mass loss, indicating the proportion of initial mass decomposed, (2) stabilisation factor (S), indicating the proportion of labile material remaining when initial decomposition has stabilised, and thus long-term carbon storage potential and (3) decomposition rate (k), indicating the rate at which labile material is lost, and thus short-term turnover[18]. We removed tea bags with experimental treatments, that increased in mass due to fungal growth, got lost, split during extraction, where labels were no longer legible or when only one site or plot was included per grid cell, resulting in a sample size of 3717 tea bags in the final analysed dataset.

We examined relationships among the three decomposition metrics, three locally-measured environmental variables (air temperature, soil temperature and soil moisture), and three gridded climate variables: air temperature and precipitation from Climatologies at High

Resolution for the Earth's Land Surface (CHELSA)[71] and European Space Agency (ESA) soil moisture data[72] using hierarchical Bayesian models. We also modelled decomposition across tundra and sub-Arctic regions[42] by extrapolating relationships using CHELSA and ESA soil moisture data from 1979 to 2013.

Site Descriptions

We established 330 decomposition sites encompassing 26 geographic regions across the circum-Arctic and alpine tundra (Table S1). Mean annual air temperatures ranged from -10.2°C to 12.7°C, with mean summer temperatures of 24.9°C at the warmest site (Alpine Japan, Site SSJ) and 3.3°C at the coldest site (Svalbard, Endalen Cassiope heath). Sites were largely above treeline though some subarctic and alpine sites extended below treeline.

Decomposition experiment

We measured decomposition using two types of tea in woven nylon mesh bags – a labile green tea and a recalcitrant rooibos tea – following the Tea Bag Index method[18]. The two tea types represent dried leaves of two shrub species (*Camellia sinensis* – green tea and *Aspalathus linearis* – rooibos tea), which strongly differ in their leaf structural and chemical traits[18,73,74]. Although these two species are not native to the tundra, their mass losses are comparable with a range of tundra species (Fig. 2), and allow comparison across sites globally[18,75]. Mass loss via leaching of these tea bags is also comparable with previous studies employing the common litter bag method (24-hour mass loss: 14% for rooibos tea and 37% for green tea, compared to 8 - 32% in litter leaching studies[76]).

We buried tea bags *in situ* at 5-8 cm depth during 2015-2017. We incubated tea for three approximate time periods – three months (summer: on average 81 days across all sites from late spring – late summer), nine months (winter: late summer to late spring) and twelve months (year: late spring to late spring). Due to the logistical constraints of accessing some field sites, not all incubations were carried out at all sites. We buried a minimum of three tea bag pairwise replicates at each site for each given period. Tea bags were buried, rather than placed on the surface, for consistency with the global standardised Tea Bag Index protocol[18]. Moreover, this increased the likelihood of recovery across the time periods covered in this study. Surface litter likely undergo greater fluctuations in temperature and moisture that may reduce decomposition[76]. Within a common site, we found that annual mass loss was greater for buried teabags compared to those in the litter layer for green tea, but not rooibos tea (Fig. S10). However, litter is commonly mixed into tundra soils through cryoturbation processes[22]. Thus, using a buried litter substrate serves as a proxy for both leaf litter decomposition when incorporated into the soil and soil organic matter decomposition[77].

We weighed tea bags prior to burial, including both the bag and tag. Upon recovery, we dried bags at 70°C for at least 48 hours, removed any attached soil or roots, and reweighed tea bags. We subtracted the mass of the bag and label to determine the mass of the tea only, and the initial masses were corrected to account for initial moisture and loss of material in transit to field sites (approximately 5.6±0.8% of mass for rooibos tea and 3.8 ± 0.4% for green tea, measured using 10 unused tea bags at three different field sites).

Decomposition variables

We calculated three metrics of decomposition: (1) overall mass loss (final tea mass divided by initial tea mass) for each tea type.

Equation 1:

$$mass\ loss = 1 - (\frac{M_t}{M_0})$$

where M_t is equal to the mass of rooibos tea at time point t (days) and M_0 is the initial mass.

(2) The stabilisation factor (*S*), which describes the proportion of potentially decomposable compounds (the hydrolysable or acid-digestible fraction, *H*) remaining upon stabilisation of decomposition. *S* is calculated using green tea, for which mass loss has stabilised within three months of burial[18] (Fig. S8), whereby:

Equation 2:

$$S = 1 - (\frac{a_g}{H_g})$$

where a_g is the decomposable fraction (mass loss) of green tea and H_g is the hydrolysable fraction of green tea.

(3) The decomposition rate (*k*), which represents the rate at which decomposable compounds are lost during decomposition. This two-pool decomposition constant was calculated based on the methods outlined in Keuskamp et al. (2013), and is calculated using rooibos tea, for which decomposition has not yet stabilised during the incubation periods covered by this analysis[18] (Fig. S8).

Equation 3:

421 $$k = ln\left(\frac{a_r}{M_{t(r)} - a_r}\right) x \frac{1}{t}$$

422 where M is equal to the mass of rooibos tea at time point t (days) and a_r is the decomposable
423 fraction of rooibos tea. a_r is calculated from the hydrolysable fraction of rooibos tea (*Hr*) and
424 stabilisation factor (*S*), whereby $a_r = H_r (1 - S)$.

425 ***Environmental variables***

426 Where possible, we measured local environmental variables at each site for the duration of
427 the incubation period. Soil temperatures were measured using digital iButtons (DS1921G
428 Thermochron iButtons, Maxim Integrated, San Jose, CA, US) or data loggers (HOBO RX3000
429 Remote Monitoring Station Data Logger, Onset Computer Corporation, Pocasset, MA; HOBO
430 Pendant temperature and light data loggers, Part # UA-002-64, Onset Computer Corporation,
431 Pocasset, MA; Lascar EL USB-1 temperature loggers, Lascar electronics, Salisbury, UK;
432 Theta Probe ML3 attached to a HH2 Moisture Meter Logger, DELTA-T-DEVICES, Cambridge,
433 UK). Soil moisture (percent volumetric water content) was measured using hand-held moisture
434 probes (Spectrum (SM100); HydroSense II; Stevens POGO probe, Stevens Water Monitoring
435 Systems Inc., Portland, OR, USA) at 5 cm depth. Where site-measured data were not
436 available, notably for air temperature, we used local weather station data, provided either by
437 the authors or additional contributors[78] and unpublished data (Annika Kristoffersson pers.
438 comm. 2017, Phil Marsh, pers. comm. 2017). All environmental data were trimmed to the
439 corresponding incubation period for analyses. Sites that did not have available local
440 environmental data were excluded from relevant analyses.
441
442 ***Gridded climate variables***

443 We used 'Climatologies at high resolution for the Earth's land surface areas' data (CHELSA,
444 0.0083 × 0.0083 degree resolution[71], http://chelsa-climate.org) to provide gridded temperature
445 and precipitation data for all sites, and to extrapolate decomposition across the tundra biome.
446 We extracted climatologies (covering the time period 1979 to 2013) for summer (June-July-
447 August), winter (December-January-February) and annual temperature and precipitation. We
448 used European Space Agency (ESA) Climate Change Initiative combined soil moisture data
449 product (0.25 × 0.25-degree resolution[72], https://www.esa-soilmoisture-cci.org) to provide
450 modelled soil moisture for all sites and to extrapolate decomposition across the tundra. We
451 used daily data for the period 1979 to 2013 to build climatologies (summer, winter, year) to
452 align with CHELSA data.
453
454 We compared site-measured environmental data to gridded climate data using hierarchical
455 Bayesian models with grid cell and site as nested random effects using the R package
456 *MCMCglmm*[79] (Fig. 3, Figs. S1-S5 and S7). Site-measured temperature variables correlated
457 closely with gridded temperature data, exhibiting a near 1:1 relationship (Fig. S11). Site-
458 measured moisture was not correlated with average ESA soil moisture data or long-term
459 CHELSA precipitation data (Fig. S11). This discrepancy may result from greater spatial and
460 inter-annual variability in moisture or precipitation compared to temperature[80], or high within-

site variation in soil moisture that is not captured by spatially variable and data-poor high-latitude precipitation records at the grid cell scale.

Environmental Relationships

We conducted three analyses of the relationships among decomposition metrics and environmental variables: (i) relationships between each individual decomposition metric and each environmental variable across all sites (Fig. 3, Figs. S1-S4), (ii) relationships between mass loss and environmental variables within each grid cell (Fig. S5) and (iii) relationships between mass loss and environmental variables accounting for interactions between temperature and moisture (Fig. S7).

Analyses of environmental relationships were conducted in the statistical programming language *Stan* run through R (v. 3.3.3 to 4.2.3) using packages *rjags*[81] (v. 4.6) and *rstan*[82] (v. 2.17.3). In all cases, models were run until convergence was reached, which was assessed both visually in trace plots and by ensuring that all Gelman–Rubin convergence diagnostic values ($\hat{R}$)[83] were less than 1.1. Code is available at:
https://github.com/ShrubHub/TundraTeaHub

Environmental Relationships – individual variables

The relationship between each decomposition metric and environmental variable was estimated from a hierarchical Bayesian model, with climatic variables as the predictor variable and decomposition as the predictor variable, with grid cell (g), site (s, unique grid referenced location) and plot (p, replicate plots within each location) as random effects, varying by tea type (t):

Equation 4:

$$decomp_{p,t} \sim Normal\left(\alpha_{p,t} + \alpha_{s,t} + \alpha_{g,t}, \sigma\right)$$

We estimated relationships with decomposition metrics over space at the level at which environmental variables were measured, including incubation length (days) as a fixed effect. For example, relationships for gridded climate data were estimated at the level of the grid cell (g), with site (s) and plot (p) as nested hierarchical random effects. Relationships for site-measured variables were estimated at the site level, with plot (p) as a random effect. If environmental variables were measured at the plot level, we summarised variables to the site level and carried forward the standard deviation among plots into models. If there was only one teabag per plot, one plot per site or one site per grid cell, $\alpha_{p,t}$ or $\alpha_{s,t}$ was set to zero. Note

that data availability differs for each environmental variable. For stabilisation factor (*S*) and decomposition rate (*k*) models, we did not vary effects by tea type (t), since only one tea type is used for each of these variables.

Equation 5:

$$\alpha_{g,t} \sim Normal(\gamma 0_t + \gamma 1_t * EV_{g,t} + \gamma 2_t * days_{g,t}, \theta)$$

$$\alpha_{p,t} \sim Normal(0, \sigma 1)$$

$$\alpha_{s,t} \sim Normal(0, \sigma 2)$$

We modelled all incubation periods separately due to large differences in the availability of environmental data and qualitative differences between conditions in different seasons such as frozen ground during the winter. ***Environmental Relationships – within grid cells***

We modelled the relationship between decomposition metrics and environmental variables (single variables only) within grid cells using the same model structure, but by standardising all environmental variables within a grid cell using mean zero and unit-variance scaling.

Environmental Relationships – temperature and moisture interactions

We modelled the relationships between mass loss and environmental variables over space accounting for both temperature and moisture within the same model (both for site-measured soil temperature and soil moisture, and for gridded air temperature and soil moisture). We used the same model structure as for individual variables, but also included an interaction term between these two environmental variables.

Equation 6:

$$\alpha_{g,t} \sim Normal(\gamma 0_t + \gamma 1_t * temp_{g,t} + \gamma 2_t * moisture_{g,t} + \gamma 3_t * temp_{g,t} * moisture_{g,t} + \gamma 4_t * days_{g,t}, \theta)$$

We ran models with environmental data in original units, and also using standardised environmental variables and incubation length using mean zero and unit-variance scaling to allow comparison across environmental variables.

Mapping decomposition

We used model estimates from the gridded climate variable model (Equation 6) to map decomposition over space based on summer temperature and moisture for tundra and subarctic climate regions. We mapped gridded temperature of the warmest quarter (CHELSA bio10) and gridded summer soil moisture (ESA, June-July-August) as environmental

variables. We used the coefficients for green tea (Fig. 5) and rooibos tea (Fig. S12), and assumed the mean incubation length across summer treatments (81 days). We masked estimates to tundra and subarctic climate regions based on the Köppen-Geiger climate classification[84] (regions ET, Dsc, Dsc, Dwc, Dwd, Dfc, Dfd). We included an estimation of global treeline based on the Circum-Arctic Vegetation Map (CAVM) classification[43].

538 **References**

539 1. Bond-Lamberty, B. & Thomson, A. Temperature-associated increases in the global soil
540 respiration record. *Nature* **464**, 579–582 (2010).

541 2. Davidson, E. A. & Janssens, I. A. Temperature sensitivity of soil carbon decomposition
542 and feedbacks to climate change. *Nature* **440**, 165–173 (2006).

543 3. Conant, R. T. *et al.* Temperature and soil organic matter decomposition rates – synthesis
544 of current knowledge and a way forward. *Glob. Change Biol.* **17**, 3392–3404 (2011).

545 4. Crowther, T. W. *et al.* Quantifying global soil carbon losses in response to warming. *Nature*
546 **540**, 104–108 (2016).

547 5. van Gestel, N. *et al.* Predicting soil carbon loss with warming. *Nature* **554**, E4–E5 (2018).

548 6. Wieder, W. R., Sulman, B. N., Hartman, M. D., Koven, C. D. & Bradford, M. A. Arctic Soil
549 Governs Whether Climate Change Drives Global Losses or Gains in Soil Carbon.
550 *Geophys. Res. Lett.* **46**, 14486–14495 (2019).

551 7. Hugelius, G. *et al.* The Northern Circumpolar Soil Carbon Database: spatially distributed
552 datasets of soil coverage and soil carbon storage in the northern permafrost regions. *Earth*
553 *Syst. Sci. Data* **5**, 3–13 (2013).

554 8. Tarnocai, C. *et al.* Soil organic carbon pools in the northern circumpolar permafrost region.
555 *Glob. Biogeochem. Cycles* **23**, (2009).

556 9. Schuur, E. A. G. *et al.* The effect of permafrost thaw on old carbon release and net carbon
557 exchange from tundra. *Nature* **459**, 556–559 (2009).

558 10. Aerts, R. The freezer defrosting: global warming and litter decomposition rates in cold
559 biomes. *J. Ecol.* **94**, 713–724 (2006).

560 11. Rantanen, M. *et al.* The Arctic has warmed nearly four times faster than the globe since
561 1979. *Commun. Earth Environ.* **3**, 1–10 (2022).

562 12. IPCC Working Group I. *Climate Change 2021: The Physical Science Basis. Contribution*
563 *of Working Group I to the Sixth Assessment Report of the Intergovernmental Panel on*
564 *Climate Change*. https://www.ipcc.ch/report/ar6/wg1/ (2021).

565 13. Schuur, E. A. G. *et al.* Climate change and the permafrost carbon feedback. *Nature* **520**,
566 171–179 (2015).

567 14. Björnsdóttir, K., Barrio, I. C. & Jónsdóttir, I. S. Long-term warming manipulations reveal
568 complex decomposition responses across different tundra vegetation types. *Arct. Sci.* 1–
569 13 (2021) doi:10.1139/as-2020-0046.

15. Cornelissen, J. H. C. *et al.* Global negative vegetation feedback to climate warming responses of leaf litter decomposition rates in cold biomes. *Ecol. Lett.* **10**, 619–627 (2007).

16. Christiansen, C. T. *et al.* Enhanced summer warming reduces fungal decomposer diversity and litter mass loss more strongly in dry than in wet tundra. *Glob. Change Biol.* **23**, 406–420 (2017).

17. Hicks Pries, C. E., Schuur, E. A. G., Vogel, J. G. & Natali, S. M. Moisture drives surface decomposition in thawing tundra. *J. Geophys. Res. Biogeosciences* **118**, 1133–1143 (2013).

18. Keuskamp, J. A., Dingemans, B. J. J., Lehtinen, T., Sarneel, J. M. & Hefting, M. M. Tea Bag Index: a novel approach to collect uniform decomposition data across ecosystems. *Methods Ecol. Evol.* **4**, 1070–1075 (2013).

19. Liski, J., Nissinen, A., Erhard, M. & Taskinen, O. Climatic effects on litter decomposition from arctic tundra to tropical rainforest. *Glob. Change Biol.* **9**, 575–584 (2003).

20. Sierra, C. A., Trumbore, S. E., Davidson, E. A., Vicca, S. & Janssens, I. Sensitivity of decomposition rates of soil organic matter with respect to simultaneous changes in temperature and moisture. *J. Adv. Model. Earth Syst.* **7**, 335–356 (2015).

21. Bonan, G. B., Hartman, M. D., Parton, W. J. & Wieder, W. R. Evaluating litter decomposition in earth system models with long-term litterbag experiments: an example using the Community Land Model version 4 (CLM4). *Glob. Change Biol.* **19**, 957–974 (2013).

22. Sistla, S. A. *et al.* Long-term warming restructures Arctic tundra without changing net soil carbon storage. *Nature* **497**, 615–618 (2013).

23. Christiansen, C. T., Mack, M. C., DeMarco, J. & Grogan, P. Decomposition of Senesced Leaf Litter is Faster in Tall Compared to Low Birch Shrub Tundra. *Ecosystems* **21**, 1564–1579 (2018).

24. Cornwell, W. K. *et al.* Plant species traits are the predominant control on litter decomposition rates within biomes worldwide. *Ecol. Lett.* **11**, 1065–1071 (2008).

25. Hobbie, S. E. Temperature and plant species control over litter decomposition in Alaskan tundra. *Ecol. Monogr.* **66**, 503–522 (1996).

26. Parker, T. C. *et al.* Exploring drivers of litter decomposition in a greening Arctic: results from a transplant experiment across a treeline. *Ecology* **99**, 2284–2294 (2018).

27. Petraglia, A. *et al.* Litter decomposition: effects of temperature driven by soil moisture and vegetation type. *Plant Soil* **435**, 187–200 (2019).

28. Fanin, N. *et al.* Relative Importance of Climate, Soil and Plant Functional Traits During the Early Decomposition Stage of Standardized Litter. *Ecosystems* **23**, 1004–1018 (2020).

29. Joly, F.-X., Scherer-Lorenzen, M. & Hättenschwiler, S. Resolving the intricate role of climate in litter decomposition. *Nat. Ecol. Evol.* **7**, 214–223 (2023).

30. Elmendorf, S. C. *et al.* Plot-scale evidence of tundra vegetation change and links to recent summer warming. *Nat. Clim. Change* **2**, 453–457 (2012).

31. García Criado, M., Myers-Smith, I. H., Bjorkman, A. D., Lehmann, C. E. R. & Stevens, N. Woody plant encroachment intensifies under climate change across tundra and savanna biomes. *Glob. Ecol. Biogeogr.* **29**, 925–943 (2020).

32. Myers-Smith, I. H. *et al.* Shrub expansion in tundra ecosystems: dynamics, impacts and research priorities. *Environ. Res. Lett.* **6**, 045509 (2011).

33. Blok, D., Elberling, B. & Michelsen, A. Initial Stages of Tundra Shrub Litter Decomposition May Be Accelerated by Deeper Winter Snow But Slowed Down by Spring Warming. *Ecosystems* **19**, 155–169 (2016).

34. Carbognani, M., Petraglia, A. & Tomaselli, M. Warming effects and plant trait control on the early-decomposition in alpine snowbeds. *Plant Soil* **376**, 277–290 (2014).

35. García-Palacios, P., Maestre, F. T., Kattge, J. & Wall, D. H. Climate and litter quality differently modulate the effects of soil fauna on litter decomposition across biomes. *Ecol. Lett.* **16**, 1045–1053 (2013).

36. Moore, T. R., Trofymow, J. A., Prescott, C. E., Fyles, J. & Titus, B. D. Patterns of Carbon, Nitrogen and Phosphorus Dynamics in Decomposing Foliar Litter in Canadian Forests. *Ecosystems* **9**, 46–62 (2006).

37. Zhang, D., Hui, D., Luo, Y. & Zhou, G. Rates of litter decomposition in terrestrial ecosystems: global patterns and controlling factors. *J. Plant Ecol.* **1**, 85–93 (2008).

38. Blume-Werry, G. *et al.* Don't drink it, bury it: comparing decomposition rates with the tea bag index is possible without prior leaching. *Plant Soil* **465**, 613–621 (2021).

39. Gallois, E. *et al.* Litter decomposition is moderated by scale-dependent microenvironmental variation in tundra ecosystems. Preprint at https://doi.org/10.32942/osf.io/crup3 (2022).

40. von Oppen, J. *et al.* Microclimate explains little variation in year-round decomposition across an Arctic tundra landscape. In: Arctic shrubs between macro- and microclimate: lessons across scales from Western Greenland. (Aarhus University, 2022).

635 41. Walker, E. R., Haydn J. D. Thomas, & Isla H. Myers-Smith. Experimental evidence of litter
636 quality and soil moisture rather than temperature as the key driver of litter decomposition
637 along a high-latitude elevational gradient. Preprint at https://doi.org/10.32942/X2M880
638 (2023).

639 42. Kottek, M., Grieser, J., Beck, C., Rudolf, B. & Rubel, F. World map of the Köppen-Geiger
640 climate classification updated. *Meteorol. Z.* **15**, 259–263 (2006).

641 43. Walker, D. A. *et al.* The Circumpolar Arctic vegetation map. *J. Veg. Sci.* **16**, 267–282
642 (2005).

643 44. Bjorkman, A. D. *et al.* Plant functional trait change across a warming tundra biome. *Nature*
644 **562**, 57–62 (2018).

645 45. Bjorkman, A. D. *et al.* Status and trends in Arctic vegetation: Evidence from experimental
646 warming and long-term monitoring. *Ambio* **49**, 678–692 (2020).

647 46. Bradford, M. A. *et al.* Climate fails to predict wood decomposition at regional scales. *Nat.*
648 *Clim. Change* **4**, 625–630 (2014).

649 47. McLaren, J. R. *et al.* Shrub encroachment in Arctic tundra: Betula nana effects on above-
650 and belowground litter decomposition. *Ecology* **98**, 1361–1376 (2017).

651 48. Buckeridge, K. M., Zufelt, E., Chu, H. & Grogan, P. Soil nitrogen cycling rates in low arctic
652 shrub tundra are enhanced by litter feedbacks. *Plant Soil* **330**, 407–421 (2010).

653 49. Mack, M. C., Schuur, E. A. G., Bret-Harte, M. S., Shaver, G. R. & Chapin, F. S. Ecosystem
654 carbon storage in Arctic tundra reduced by long-term nutrient fertilization. *Nature* **431**,
655 440–443 (2004).

656 50. Clemmensen, K. E. *et al.* A tipping point in carbon storage when forest expands into tundra
657 is related to mycorrhizal recycling of nitrogen. *Ecol. Lett.* **24**, 1193–1204 (2021).

658 51. Hicks, L. C., Yuan, M., Brangarí, A., Rousk, K. & Rousk, J. Increased Above- and
659 Belowground Plant Input Can Both Trigger Microbial Nitrogen Mining in Subarctic Tundra
660 Soils. *Ecosystems* **25**, 105–121 (2022).

661 52. Moorhead, D. L. & Sinsabaugh, R. L. A Theoretical Model of Litter Decay and Microbial
662 Interaction. *Ecol. Monogr.* **76**, 151–174 (2006).

663 53. Keuper, F. *et al.* Carbon loss from northern circumpolar permafrost soils amplified by
664 rhizosphere priming. *Nat. Geosci.* **13**, 560–565 (2020).

665 54. Street, L. E. *et al.* Plant carbon allocation drives turnover of old soil organic matter in
666 permafrost tundra soils. *Glob. Change Biol.* **26**, 4559–4571 (2020).

667 55. Wardle, D. A. *et al.* Ecological Linkages Between Aboveground and Belowground Biota.
668 *Science* **304**, 1629–1633 (2004).

669 56. Knorr, M., Frey, S. D. & Curtis, P. S. Nitrogen Additions and Litter Decomposition: A Meta-
670 Analysis. *Ecology* **86**, 3252–3257 (2005).

671 57. Thakur, M. P. *et al.* Reduced feeding activity of soil detritivores under warmer and drier
672 conditions. *Nat. Clim. Change* **8**, 75–78 (2018).

673 58. Rinnan, R., Michelsen, A. & Jonasson, S. Effects of litter addition and warming on soil
674 carbon, nutrient pools and microbial communities in a subarctic heath ecosystem. *Appl.*
675 *Soil Ecol.* **39**, 271–281 (2008).

676 59. Koltz, A. M., Schmidt, N. M. & Høye, T. T. Differential arthropod responses to warming are
677 altering the structure of Arctic communities. *R. Soc. Open Sci.* **5**, 171503 (2018).

678 60. Peng, Y. *et al.* Soil fauna effects on litter decomposition are better predicted by fauna
679 communities within litterbags than by ambient soil fauna communities. *Plant Soil* (2023)
680 doi:10.1007/s11104-023-05902-1.

681 61. Xue, K. *et al.* Tundra soil carbon is vulnerable to rapid microbial decomposition under
682 climate warming. *Nat. Clim. Change* **6**, 595–600 (2016).

683 62. Lara, M. J. *et al.* Local-scale Arctic tundra heterogeneity affects regional-scale carbon
684 dynamics. *Nat. Commun.* **11**, 4925 (2020).

685 63. Lind, L., Harbicht, A., Bergman, E., Edwartz, J. & Eckstein, R. L. Effects of initial leaching
686 for estimates of mass loss and microbial decomposition—Call for an increased nuance.
687 *Ecol. Evol.* **12**, e9118 (2022).

688 64. Canessa, R. *et al.* Relative effects of climate and litter traits on decomposition change with
689 time, climate and trait variability. *J. Ecol.* **109**, 447–458 (2021).

690 65. Harmon, M. E. *et al.* Long-term patterns of mass loss during the decomposition of leaf and
691 fine root litter: an intersite comparison. *Glob. Change Biol.* **15**, 1320–1338 (2009).

692 66. Hollister, R. D., Webber, P. J. & Tweedie, C. E. The response of Alaskan arctic tundra to
693 experimental warming: differences between short- and long-term responses. *Glob.*
694 *Change Biol.* **11**, 525–536 (2005).

695 67. Trofymow, J. A. *et al.* Rates of litter decomposition over 6 years in Canadian forests:
696 influence of litter quality and climate. *Can. J. For. Res.* **32**, 789–804 (2002).

697 68. Macias-Fauria, M., Seddon, A. W. R., Benz, D., Long, P. R. & Willis, K. Spatiotemporal
698 patterns of warming. *Nat. Clim. Change* **4**, 845–846 (2014).

699 69. Althuizen, I. H. J., Lee, H., Sarneel, J. M. & Vandvik, V. Long-Term Climate Regime
700 Modulates the Impact of Short-Term Climate Variability on Decomposition in Alpine
701 Grassland Soils. *Ecosystems* **21**, 1580–1592 (2018).

702 70. Virkkala, A.-M. *et al.* Statistical upscaling of ecosystem CO2 fluxes across the terrestrial
703 tundra and boreal domain: Regional patterns and uncertainties. *Glob. Change Biol.* **27**,
704 4040–4059 (2021).

705 71. Karger, D. N. *et al.* Climatologies at high resolution for the earth's land surface areas. *Sci.*
706 *Data* **4**, 170122 (2017).

707 72. Dorigo, W. *et al.* ESA CCI Soil Moisture for improved Earth system understanding: State-
708 of-the art and future directions. *Remote Sens. Environ.* **203**, 185–215 (2017).

709 73. Graham, H. N. Green tea composition, consumption, and polyphenol chemistry. *Prev.*
710 *Med.* **21**, 334–350 (1992).

711 74. Krafczyk, N. & Glomb, M. A. Characterization of Phenolic Compounds in Rooibos Tea. *J.*
712 *Agric. Food Chem.* **56**, 3368–3376 (2008).

713 75. Djukic, I. *et al.* Early stage litter decomposition across biomes. *Sci. Total Environ.* **628–**
714 **629**, 1369–1394 (2018).

715 76. Bokhorst, S., Bjerke, J. W., Melillo, J., Callaghan, T. V. & Phoenix, G. K. Impacts of
716 extreme winter warming events on litter decomposition in a sub-arctic heathland. *Soil Biol.*
717 *Biochem.* **42**, 611–617 (2010).

718 77. Eskelinen, A., Stark, S. & Männistö, M. Links between plant community composition, soil
719 organic matter quality and microbial communities in contrasting tundra habitats. *Oecologia*
720 **161**, 113–123 (2009).

721 78. Niittynen, P. *et al.* Fine-scale tundra vegetation patterns are strongly related to winter
722 thermal conditions. *Nat. Clim. Change* **10**, 1143–1148 (2020).

723 79. Hadfield, J. D. MCMC Methods for Multi-Response Generalized Linear Mixed Models: The
724 MCMCglmm R Package. **33**, 1–22 (2010).

725 80. Seneviratne, S. I. *et al.* Investigating soil moisture–climate interactions in a changing
726 climate: A review. *Earth-Sci. Rev.* **99**, 125–161 (2010).

727 81. Plummer, M. rjags: Bayesian Graphical Models using MCMC. (2016).

728 82. Stan Development Team. RStan: the R interface to Stan. (2018).

729 83. Gelman, A. & Rubin, D. B. Inference from Iterative Simulation Using Multiple Sequences.
730 *Stat. Sci.* **7**, 457–472 (1992).

84. Peel, M. C., Finlayson, B. L. & McMahon, T. A. Updated world map of the Köppen-Geiger climate classification. *Hydrol. Earth Syst. Sci.* **11**, 1633–1644 (2007).

Supplementary Tables

Table S1. Summary of geographic locations used in main study, indicating number of sites and plots (the base study unit), number of tea bag replicates used in study, and mean temperatures (CHELSA data 1979-2013, summer = warmest quarter, winter = coldest quarter).

Geographic Region	Number of sites	Number of plots	Number of tea bags	Mean temperature (°C) (year / summer / winter)		
Alpine Japan	45	46	776	6.7	18.7	-4.5
Auðkúluheiði, Iceland	3	3	110	0.9	8.6	-5.0
Australian Alps	1	18	191	4.7	11.4	-1.5
Disko Island, Greenland	7	7	112	-4.0	7.1	-15.4
Fairbanks, Alaska	7	14	56	-4.8	14.3	-22.0
Kilpisjärvi, Finland	82	120	751	-2.1	10.2	-13.2
Gothic Mountain, Colorado, USA	5	5	95	2.2	13.4	-8.1
Italian Alps	2	14	116	-1.6	7.5	-10.1
Kangerlussuaq, Greenland	2	2	36	-5.6	7.5	-16.6
Khanymey, western Siberia	2	2	15	-3.6	15.4	-21.1
Kluane, Yukon, Canada	15	72	757	-3.1	8.8	-14.1
Lofoten Islands, Norway	1	16	55	5.8	12.6	0.8
Narsarsuaq, Greenland	10	49	450	-3.3	6.6	-12.0
Northern Norway	35	62	119	0.5	11.9	-9.7
Northern Sweden	56	122	467	-2.1	9.9	-12.8
Qikiqtaruk-Herschel Island, Yukon, Canada	9	14	224	-9.4	7.6	-24.3
Southampton Island, Nunavut, Canada	1	1	5	-9.4	6.4	-26.6
Svalbard	25	109	468	-6.3	4.2	-14.7
Swiss Alps	3	61	256	-1.00	8.0	-9.4
Þeistareykir, Iceland	2	2	72	1.7	8.9	-3.5
Þingvellir, Iceland	1	1	40	4.0	10.7	-1.1
Tazovsky, western Siberia	1	1	8	-7.4	12.5	-25.1
Toolik Lake, Alaska, USA	2	7	140	-10.2	10.4	-26.6
Trail Valley, NWT, Canada	10	30	180	-9.1	12.0	-27.2
Umiujaq, Québec, Canada	2	2	40	-3.9	9.9	-20.8
Urengoy, western Siberia	1	1	8	-6.3	13.7	-24.0

Table S2. Model outputs for individual environmental variable – decomposition relationships. Bold rows designate relationships (slope parameter) for which the credible interval does not cross zero (i.e., the relationship is "significant"). Sample size indicates number of tea samples available to test relationships. Effective sample size indicates number of convergent model runs. G and R indicate green and rooibos tea, respectively.

Environ. Variable	Decomp. variable	Time period	Tea Type	Parameter	Mean	SD	2.50%	97.50%	Sample size	Effective sample size
Air temp. (measured)	Mass loss	Summer	G	Intercept	0.531	0.006	0.519	0.543	1913	15 000
Air temp. (measured)	Mass loss	Summer	R	Intercept	0.17	0.006	0.158	0.182	1913	15 000
Air temp. (measured)	**Mass loss**	**Summer**	**G**	**Slope**	**0.008**	**0.002**	**0.004**	**0.012**	**1913**	**15 000**
Air temp. (measured)	**Mass loss**	**Summer**	**R**	**Slope**	**0.005**	**0.002**	**0.001**	**0.004**	**1913**	**15 000**
Soil temp. (measured)	Mass loss	Summer	G	Intercept	0.605	0.006	0.593	0.616	1560	15 000
Soil temp. (measured)	Mass loss	Summer	R	Intercept	0.22	0.006	0.208	0.231	1560	15 000
Soil temp. (measured)	**Mass loss**	**Summer**	**G**	**Slope**	**0.02**	**0.002**	**0.017**	**0.023**	**1560**	**15 000**
Soil temp. (measured)	**Mass loss**	**Summer**	**R**	**Slope**	**0.011**	**0.002**	**0.008**	**0.014**	**1560**	**15 000**
Moisture (measured)	Mass loss	Summer	G	Intercept	0.523	0.009	0.504	0.541	917	15 000
Moisture (measured)	Mass loss	Summer	R	Intercept	0.183	0.009	0.165	0.201	917	15 000
Moisture (measured)	**Mass loss**	**Summer**	**G**	**Slope**	**7.36E-04**	**3.75E-04**	**1.45E-05**	**1.47E-03**	**917**	**14 142**
Moisture (measured)	Mass loss	Summer	R	Slope	7.16E-05	3.68E-04	-6.57E-04	8.09E-04	917	15 000
Air temp. (CHELSA)	Mass loss	Summer	G	Intercept	0.559	0.009	0.541	0.577	2837	15 000
Air temp. (CHELSA)	Mass loss	Summer	R	Intercept	0.204	0.009	0.187	0.222	2837	15 000
Air temp. (CHELSA)	**Mass loss**	**Summer**	**G**	**Slope**	**0.017**	**0.002**	**0.013**	**0.021**	**2837**	**7178**
Air temp. (CHELSA)	**Mass loss**	**Summer**	**R**	**Slope**	**0.012**	**0.002**	**0.008**	**0.015**	**2837**	**15 000**
Precip. (CHELSA)	Mass loss	Summer	G	Intercept	0.565	0.01	0.545	0.585	2837	15 000
Precip. (CHELSA)	Mass loss	Summer	R	Intercept	0.209	0.01	0.19	0.229	2837	15 000
Precip. (CHELSA)	**Mass loss**	**Summer**	**G**	**Slope**	**0.004**	**0.001**	**0.003**	**0.005**	**2837**	**15 000**
Precip. (CHELSA)	**Mass loss**	**Summer**	**R**	**Slope**	**0.003**	**0.001**	**0.003**	**0.004**	**2837**	**15 000**
Moisture (ESA)	Mass loss	Summer	G	Intercept	0.595	0.013	0.569	0.621	2234	15 000
Moisture (ESA)	Mass loss	Summer	R	Intercept	0.232	0.013	0.206	0.258	2234	15 000
Moisture (ESA)	**Mass loss**	**Summer**	**G**	**Slope**	**0.013**	**0.004**	**0.005**	**0.02**	**2234**	**15 000**
Moisture (ESA)	Mass loss	Summer	R	Slope	0.007	0.004	-9.38E-05	0.015	2234	15 000
Air temp. (measured)	Mass loss	Winter	G	Intercept	0.561	0.03	0.503	0.621	176	15 000
Air temp. (measured)	Mass loss	Winter	R	Intercept	0.226	0.031	0.165	0.287	176	15 000
Air temp. (measured)	**Mass loss**	**Winter**	**G**	**Slope**	**0.044**	**0.016**	**0.012**	**0.074**	**176**	**15 000**
Air temp. (measured)	Mass loss	Winter	R	Slope	-0.002	0.016	-0.033	0.029	176	15 000

Soil temp. (measured)	Mass loss	Winter	G	Intercept	0.498	0.041	0.416	0.58	71	5842
Soil temp. (measured)	Mass loss	Winter	R	Intercept	0.195	0.113	0.113	0.278	71	15 000
Soil temp. (measured)	Mass loss	Winter	G	Slope	0.003	0.008	-0.013	0.019	71	7964
Soil temp. (measured)	Mass loss	Winter	R	Slope	0.004	0.008	-0.012	0.02	71	15 000
Moisture (measured)	Mass loss	Winter	G	Intercept	0.553	0.007	0.538	0.567	206	9488
Moisture (measured)	Mass loss	Winter	R	Intercept	0.19	0.007	0.175	0.204	206	8980
Moisture (measured)	Mass loss	Winter	G	Slope	0.001	0.001	-1.51E-05	0.002	206	12 291
Moisture (measured)	Mass loss	Winter	R	Slope	4.42E-04	0.001	-5.93E-04	0.001	206	15 000
Air temp. (CHELSA)	Mass loss	Winter	G	Intercept	0.542	0.005	0.451	0.637	427	15 000
Air temp. (CHELSA)	Mass loss	Winter	R	Intercept	0.208	0.005	0.116	0.3	427	15 000
Air temp. (CHELSA)	Mass loss	Winter	G	Slope	0.019	0.012	-0.006	0.043	427	15 000
Air temp. (CHELSA)	Mass loss	Winter	R	Slope	-3.47E-05	0.012	-0.024	0.024	427	15 000
Precip. (CHELSA)	Mass loss	Winter	G	Intercept	0.54	0.046	0.453	0.634	427	15 000
Precip. (CHELSA)	Mass loss	Winter	R	Intercept	0.206	0.046	0.114	0.299	427	15 000
Precip. (CHELSA)	Mass loss	Winter	G	Slope	0.005	0.003	-0.001	0.011	427	15 000
Precip. (CHELSA)	Mass loss	Winter	R	Slope	-4.88E-04	0.003	-0.007	0.006	427	15 000
Moisture (ESA)	Mass loss	Winter	G	Intercept	0.541	0.045	0.451	0.633	309	15 000
Moisture (ESA)	Mass loss	Winter	R	Intercept	0.207	0.046	0.118	0.298	309	15 000
Moisture (ESA)	**Mass loss**	**Winter**	**G**	**Slope**	**0.073**	**0.032**	**0.008**	**0.137**	**309**	**15 000**
Moisture (ESA)	Mass loss	Winter	R	Slope	-0.01	0.033	-0.075	0.054	309	15 000
Air temp. (measured)	Mass loss	Year	G	Intercept	0.581	0.006	0.578	0.6	1251	15 000
Air temp. (measured)	Mass loss	Year	R	Intercept	0.228	0.006	0.217	0.24	1251	15 000
Air temp. (measured)	**Mass loss**	**Year**	**G**	**Slope**	**0.011**	**0.002**	**0.007**	**0.015**	**1251**	**15 000**
Air temp. (measured)	**Mass loss**	**Year**	**R**	**Slope**	**0.014**	**0.002**	**0.01**	**0.018**	**1251**	**15 000**
Soil temp. (measured)	Mass loss	Year	G	Intercept	0.591	0.014	0.564	0.619	342	15 000
Soil temp. (measured)	Mass loss	Year	R	Intercept	0.263	0.014	0.237	0.29	342	15 000
Soil temp. (measured)	**Mass loss**	**Year**	**G**	**Slope**	**0.018**	**0.004**	**0.011**	**0.027**	**342**	**15 000**
Soil temp. (measured)	**Mass loss**	**Year**	**R**	**Slope**	**0.019**	**0.004**	**0.011**	**0.027**	**342**	**15 000**
Moisture (measured)	Mass loss	Year	G	Intercept	0.614	0.005	0.604	0.625	760	15 000
Moisture (measured)	Mass loss	Year	R	Intercept	0.255	0.006	0.245	0.266	760	15 000
Moisture (measured)	Mass loss	Year	G	Slope	-0.001	3.89E-04	-0.001	1.54E-04	760	15 000
Moisture (measured)	Mass loss	Year	R	**Slope**	**-0.001**	**4.06E-04**	**-0.002**	**1.06E-04**	**760**	**15 000**
Air temp. (CHELSA)	Mass loss	Year	G	Intercept	0.606	0.011	0.585	0.628	1377	15 000
Air temp. (CHELSA)	Mass loss	Year	R	Intercept	0.236	0.011	0.215	0.258	1377	15 000
Air temp. (CHELSA)	**Mass loss**	**Year**	**G**	**Slope**	**0.015**	**0.003**	**0.009**	**0.02**	**1377**	**10 775**

Air temp. (CHELSA)	**Mass loss**	**Year**	**R**	**Slope**	**0.01**	**0.003**	**0.004**	**0.015**	**1377**	**9975**
Precip. (CHELSA)	Mass loss	Year	G	Intercept	0.601	0.015	0.572	0.631	1377	15 000
Precip. (CHELSA)	Mass loss	Year	R	Intercept	0.236	0.015	0.207	0.265	1377	15 000
Precip. (CHELSA)	**Mass loss**	**Year**	**G**	**Slope**	**0.001**	**4.15E-04**	**2.48E-04**	**0.002**	**1377**	**15 000**
Precip. (CHELSA)	Mass loss	Year	R	Slope	3.06E-04	4.05E-04	-5.02E-04	0.001	1377	15 000
Moisture (ESA)	Mass loss	Year	G	Intercept	0.62	0.017	0.588	0.655	1098	15 000
Moisture (ESA)	Mass loss	Year	R	Intercept	0.252	0.017	0.219	0.285	1098	15 000
Moisture (ESA)	Mass loss	Year	G	Slope	0.008	0.004	-4.67E-05	0.015	1098	15 000
Moisture (ESA)	Mass loss	Year	R	Slope	0.005	0.004	-2.84E-03	0.007	1098	15 000
Air temp. (measured)	k	Summer	R	Intercept	0.011	3.89E-04	0.01	0.012	927	15 000
Air temp. (measured)	**k**	**Summer**	**R**	**Slope**	**4.28E-04**	**1.36E-04**	**1.59E-04**	**6.97E-04**	**927**	**15 000**
Soil temp. (measured)	k	Summer	R	Intercept	0.011	3.29E-04	0.01	0.011	704	15 000
Soil temp. (measured)	k	Summer	R	Slope	1.46E-04	8.92E-05	-2.85E-05	3.20E-04	704	15,000
Moisture (measured)	k	Summer	R	Intercept	0.012	0.001	0.011	0.013	398	15 000
Moisture (measured)	k	Summer	R	Slope	-3.97E-05	2.54E-05	-9.01E-05	9.95E-06	398	15 000
Air temp. (CHELSA)	k	Summer	R	Intercept	0.011	0.001	0.01	0.012	1403	15 000
Air temp. (CHELSA)	k	Summer	R	Slope	1.72E-04	1.20E-04	-6.58E-05	4.08E-04	1403	15 000
Precip. (CHELSA)	k	Summer	R	Intercept	0.011	0.001	0.01	0.012	1403	15 000
Precip. (CHELSA)	k	Summer	R	Slope	1.07E-05	3.22E-05	-5.23E-05	7.35E-05	1403	15 000
Moisture (ESA)	k	Summer	R	Intercept	0.011	0.001	0.01	0.012	1108	15 000
Moisture (ESA)	k	Summer	R	Slope	-7.21E-07	1.23E-06	-2.90E-04	3.02E-04	1108	15 000
Air temp. (measured)	S	Summer	G	Intercept	0.372	0.009	0.366	0.39	944	15 000
Air temp. (measured)	**S**	**Summer**	**G**	**Slope**	**-0.007**	**0.003**	**-0.014**	**-9.41E-04**	**944**	**15 000**
Soil temp. (measured)	S	Summer	G	Intercept	0.327	0.009	0.309	0.346	715	15 000
Soil temp. (measured)	**S**	**Summer**	**G**	**Slope**	**-0.026**	**0.002**	**-0.031**	**-0.021**	**715**	**15 000**
Moisture (measured)	S	Summer	G	Intercept	0.373	0.015	0.344	0.403	408	15 000
Moisture (measured)	**S**	Summer	G	Slope	-0.001	4.67E-06	-0.002	8.67E-06	408	15 000
Air temp. (CHELSA)	S	Summer	G	Intercept	0.364	0.013	0.338	0.39	1436	8376
Air temp. (CHELSA)	**S**	**Summer**	**G**	**Slope**	**-0.021**	**0.003**	**-0.026**	**-0.016**	**1436**	**8560**
Precip. (CHELSA)	S	Summer	G	Intercept	0.355	0.015	0.326	0.384	1436	15 000
Precip. (CHELSA)	**S**	**Summer**	**G**	**Slope**	**-0.005**	**0.001**	**-0.007**	**-0.004**	**1436**	**15 000**
Moisture (ESA)	S	Summer	G	Intercept	0.297	0.019	0.258	0.334	1128	15 000
Moisture (ESA)	**S**	**Summer**	**G**	**Slope**	**-0.019**	**0.005**	**-0.029**	**-0.008**	**1128**	**15 000**

746

Table S3. Model outputs for environmental variable – decomposition relationships within grid cells. Bold rows designate relationships (slope parameter) for which the credible interval does not cross zero (i.e., the relationship is "significant"). Sample size indicates number of tea samples available to test relationships. Effective sample size indicates number of convergent model runs. Variables are standardised within grid cells using mean zero and unit-variance scaling. All models are for summer incubations only. G and R indicate green and rooibos tea, respectively.

Environmental variable	Decomp variable	Tea Type	Parameter	Mean	SD	2.5%	97.5%	Sample size	Effective sample size
Air temp.	Mass loss	G	Intercept	0.815	0.112	0.595	1.033	1504	4865
Air temp.	Mass loss	R	Intercept	-0.996	0.111	-1.215	-0.782	1504	5131
Air temp.	Mass loss	G	Slope	-0.029	0.036	-0.100	0.041	1504	1964
Air temp.	Mass loss	R	Slope	0.033	0.026	-0.034	0.066	1504	4794
Soil temp.	Mass loss	G	Intercept	0.856	0.122	0.616	1.088	1311	230
Soil temp.	Mass loss	R	Intercept	-0.822	0.120	-1.061	-0.588	1311	137
Soil temp.	**Mass loss**	**G**	**Slope**	**0.144**	**0.027**	**0.091**	**0.197**	**1446**	**261**
Soil temp.	**Mass loss**	**R**	**Slope**	**0.073**	**0.026**	**0.021**	**0.122**	**1446**	**420**
Moisture	Mass loss	G	Intercept	0.816	0.164	0.492	1.132	802	597
Moisture	Mass loss	R	Intercept	-0.877	0.161	-1.191	-0.565	802	817
Moisture	Mass loss	G	Slope	0.049	0.052	-0.054	0.153	802	368
Moisture	Mass loss	R	Slope	0.059	0.046	-0.034	0.151	802	657

Table S4. Model outputs for temperature – decomposition relationships, including an interaction with soil moisture. Bold rows designate relationships (slope parameter) for which the credible interval does not cross zero (i.e., the relationship is "significant"). Sample size indicates number of tea samples available to test relationships. Effective sample size indicates number of convergent model runs. Environmental variables are unscaled and in original units. All models are for summer incubations only. G and R indicate green and rooibos tea, respectively.

Environmental. variable	Decomp. variable	Tea Type	Parameter	Mean	SD	2.5%	97.5%	Sample size	Effective sample size
Measured soil temp. × moisture	Mass loss	G	Intercept	0.522	0.018	0.487	0.558	624	5009
Measured soil temp. × moisture	**Mass loss**	**G**	**Temp. slope**	**0.029**	**0.008**	**0.014**	**0.044**	**624**	**4470**
Measured soil temp. × moisture	**Mass loss**	**G**	**Moisture slope**	**0.002**	**0.001**	**0.001**	**0.004**	**624**	**6430**
Measured soil temp. × moisture	Mass loss	G	Interaction	-1.38e-04	3.32e-04	-5.35e-04	7.86e-04	624	6277
Measured soil temp. × moisture	Mass loss	R	Intercept	0.176	0.016	0.144	0.209	624	6799
Measured soil temp. × moisture	Mass loss	R	Temp. slope	0.008	0.007	-0.004	0.022	624	6349
Measured soil temp. × moisture	Mass loss	R	Moisture slope	0.001	0.001	-0.001	0.002	624	8261
Measured soil temp. × moisture	Mass loss	R	Interaction	4.97e-05	2.81e-04	-5.07e-04	6.05e-04	624	7942
Gridded temp. × moisture	Mass loss	G	Intercept	0.581	0.009	0.563	0.599	2,234	15 000
Gridded temp. × moisture	**Mass loss**	**G**	**Temp. slope**	**0.019**	**0.002**	**0.015**	**0.023**	**2,234**	**15 000**
Gridded temp. × moisture	**Mass loss**	**G**	**Moisture slope**	**0.009**	**0.003**	**0.004**	**0.014**	**2,234**	**15 000**
Gridded temp. × moisture	Mass loss	G	Interaction	0.001	0.001	-6.39e-04	0.002	2,234	15 000
Gridded temp. × moisture	Mass loss	R	Intercept	0.218	0.009	0.201	0.234	2,234	15 000
Gridded temp. × moisture	**Mass loss**	**R**	**Temp. slope**	**0.012**	**0.002**	**0.008**	**0.015**	**2,234**	**15 000**
Gridded temp. × moisture	Mass loss	R	Moisture slope	0.004	0.002	-0.001	0.009	2,234	15 000
Gridded temp. × moisture	**Mass loss**	**R**	**Interaction**	**0.001**	**0.001**	**2.67e-05**	**0.003**	**2,234**	**15 000**

Table S5. Model outputs for relationships between measured environmental variables and gridded environmental variables. Bold rows designate relationships (slope parameter) for which the credible interval does not cross zero (i.e., the relationship is "significant"). Sample size indicates number of sites available to test relationships. Effective sample size indicates number of convergent model runs.

Measured variable	Gridded variable	Parameter	Mean	2.5%	97.5%	Sample size	Effective sample size
Air temperature	CHELSA air temperature	Intercept	-0.225	-1.596	1.194	151	15 000
Air temperature	**CHELSA air temperature**	**Slope**	**0.877**	**0.474**	**1.013**	**151**	**15 000**
Soil temperature	CHELSA air temperature	Intercept	-2.259	-3.507	-1.013	134	15 000
Soil temperature	**CHELSA air temperature**	**Slope**	**1.24**	**1.130**	**1.352**	**134**	**15 000**
Soil moisture	CHELSA precipitation	Intercept	16.876	14.625	19.197	79	15 000
Soil moisture	**CHELSA precipitation**	**Slope**	**-0.120**	**-0.170**	**-0.074**	**79**	**11 445**
Soil moisture	ESA soil moisture	Intercept	24.405	22.237	26.612	39	15 000
Soil moisture	ESA soil moisture	Slope	0.061	-0.004	0.128	39	15 000

Supplementary Figures

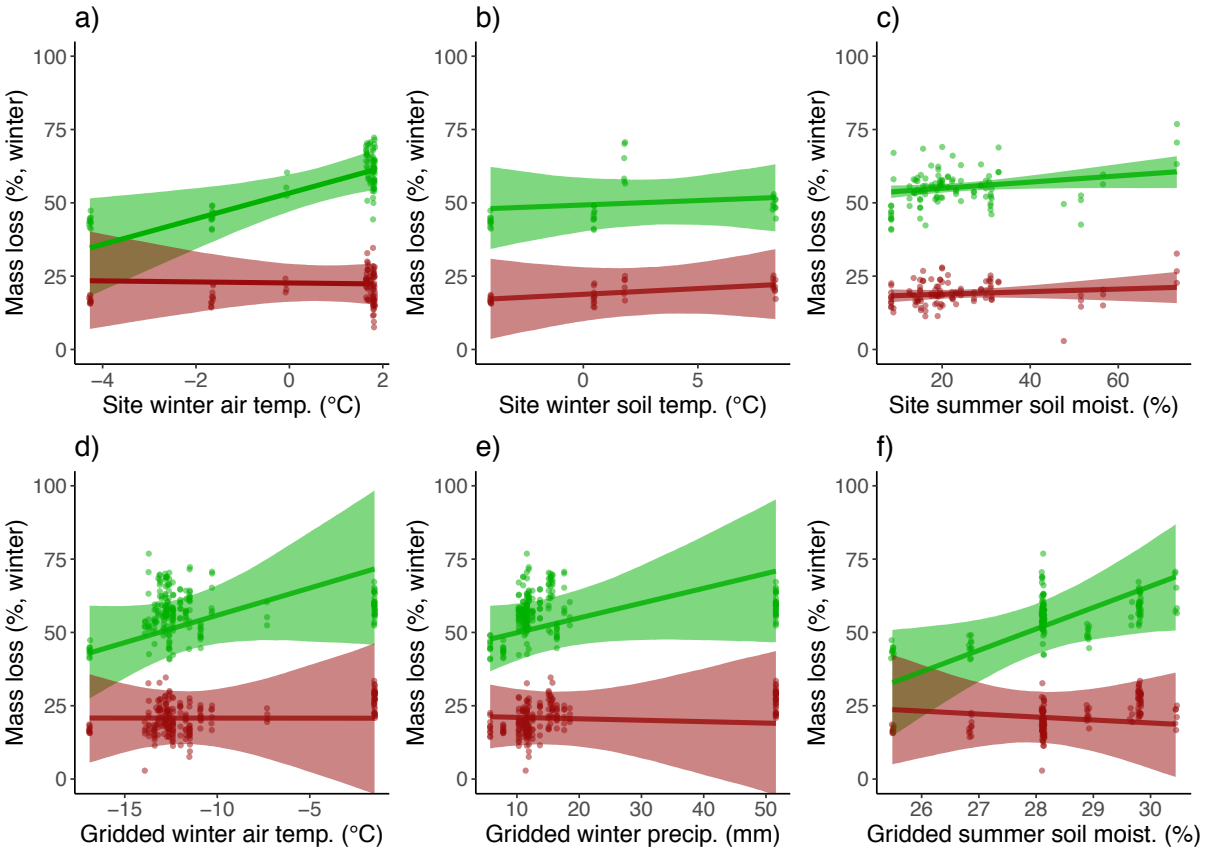

Figure S1. Relationships between decomposition (mass loss), measured environmental variables (a-c) and gridded climate data (d-f) for winter tea incubations, as opposed to summer incubations in main text (Fig. 3) or year-long incubations (Fig. S2). Points indicate individual tea bag replicates across all sites. Lines indicate hierarchical Bayesian model fits with 97.5% credible intervals. Colours indicate tea type (red = rooibos tea, green = green tea). See Table S2 for model outputs.

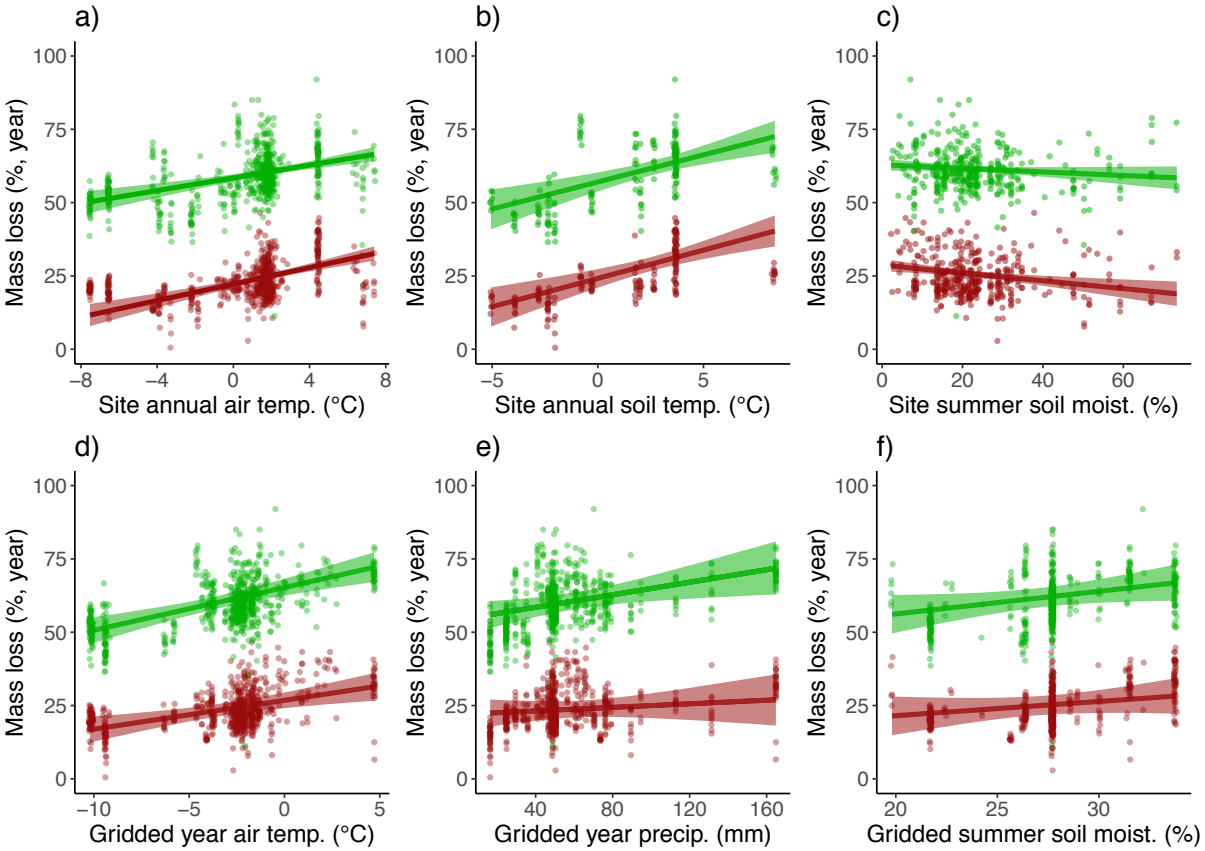

Figure S2. Relationships between decomposition (mass loss), measured environmental variables (a-c) and gridded climate data (d-f) for year-long tea incubations, as opposed to summer incubations in main text (Fig. 3) or winter incubations (Fig. S1). Points indicate individual tea bag replicates across all sites. Lines indicate hierarchical Bayesian model fits with 97.5% credible intervals. Colours indicate tea type (red = rooibos tea, green = green tea). See Table S2 for model outputs.

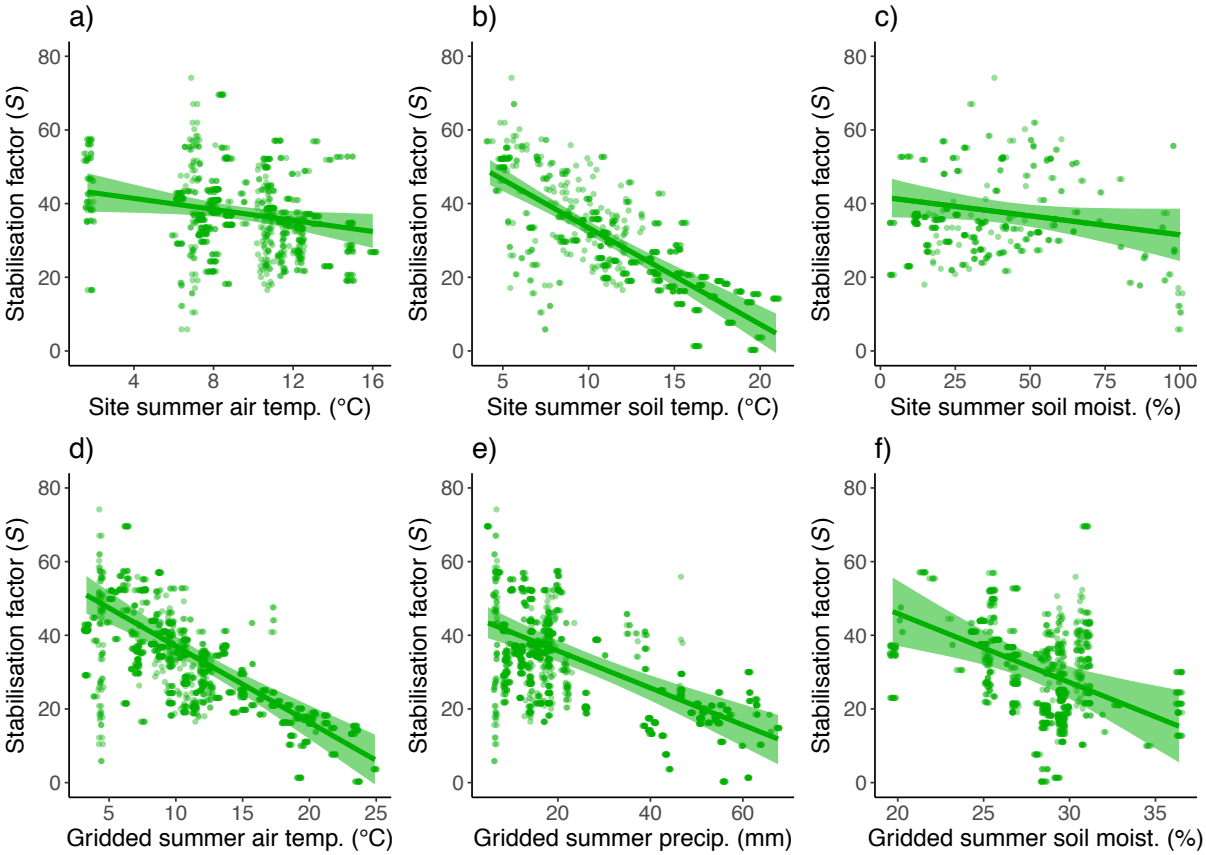

Figure S3. Relationships between stabilisation factor (*S*), measured environmental variables (a-c) and gridded climate data (d-f) for summer tea incubations, as opposed to summer mass loss in main text (Fig. 3). *S* is calculated based on decomposition of green tea, and is assumed to be consistent across tea types[18]. *S* represents the proportion of labile material remaining once decomposition has stabilised, and thus long-term carbon storage. Points indicate individual tea bag replicates across all sites. Lines indicate hierarchical Bayesian model fits with 97.5% credible intervals. See Table S2 for model outputs.

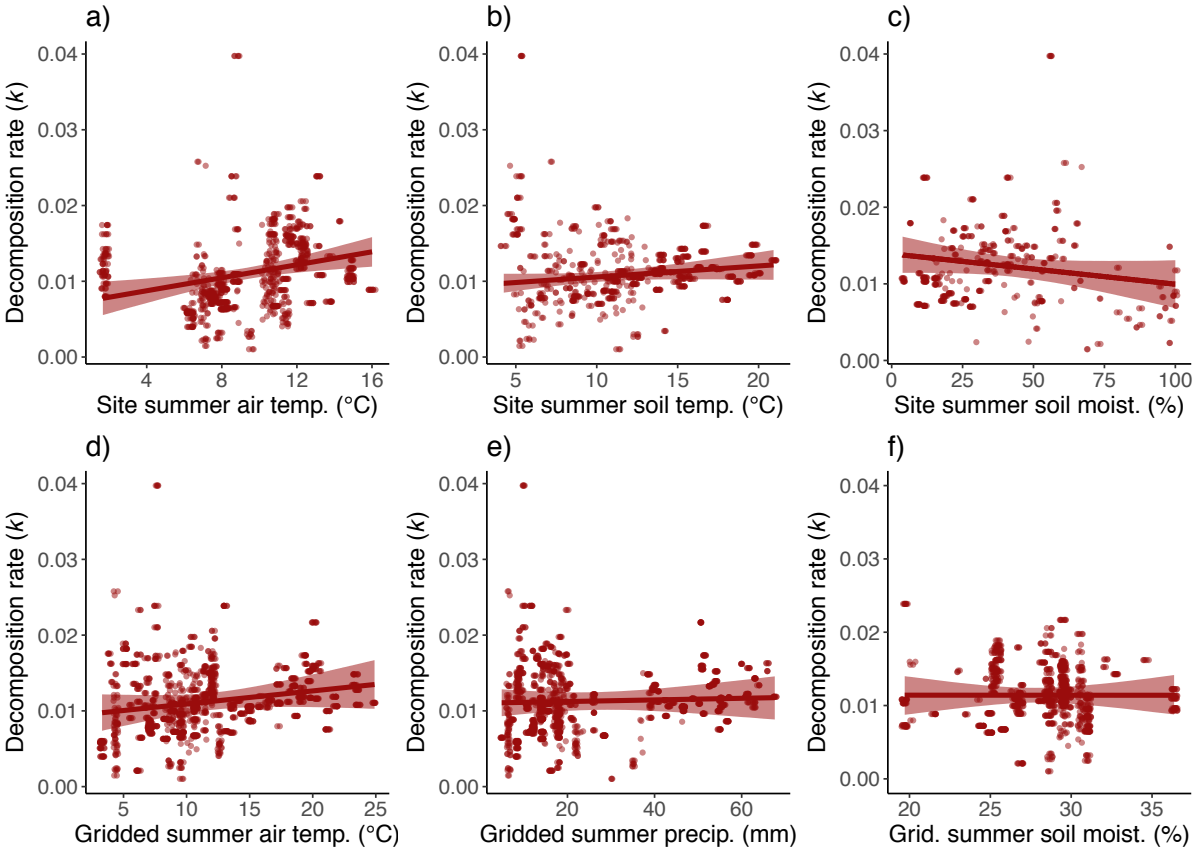

Figure S4. Relationships between decomposition rate (*k*), measured environmental variables (a-c) and gridded climate data (d-f) for summer tea incubations, as opposed to summer mass loss in main text (Fig. 3). *k* is calculated based on decomposition of rooibos tea, and is assumed to be consistent across tea types[18]. *k* represents the rate of loss of labile material, and thus short-term decomposition dynamics and biogeochemical cycling. Points indicate individual tea bag replicates across all sites. Lines indicate hierarchical Bayesian model fits with 97.5% credible intervals. See Table S2 for model outputs.

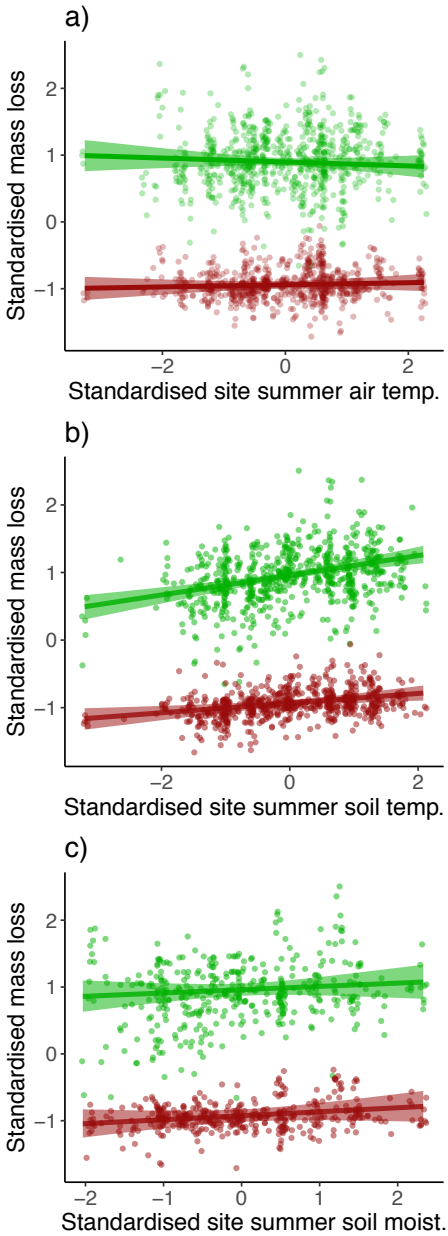

Figure S5. Within-grid cell relationships reflect among-site relationships between environmental variables and mass loss, but with greater variability. Within-grid cell relationships between summer decomposition (mass loss) and measured environmental variables, as opposed to among sites in main text (Fig. 3). Environmental and decomposition variables are standardised within 0.25 × 0.25-degree resolution grid cells using mean zero and unit-variance scaling. Points indicate individual tea bag replicates. Lines indicate hierarchical Bayesian model fits with 97.5% credible intervals. Colours indicate tea type (red = rooibos tea, green = green tea). See Table S3 for model outputs.

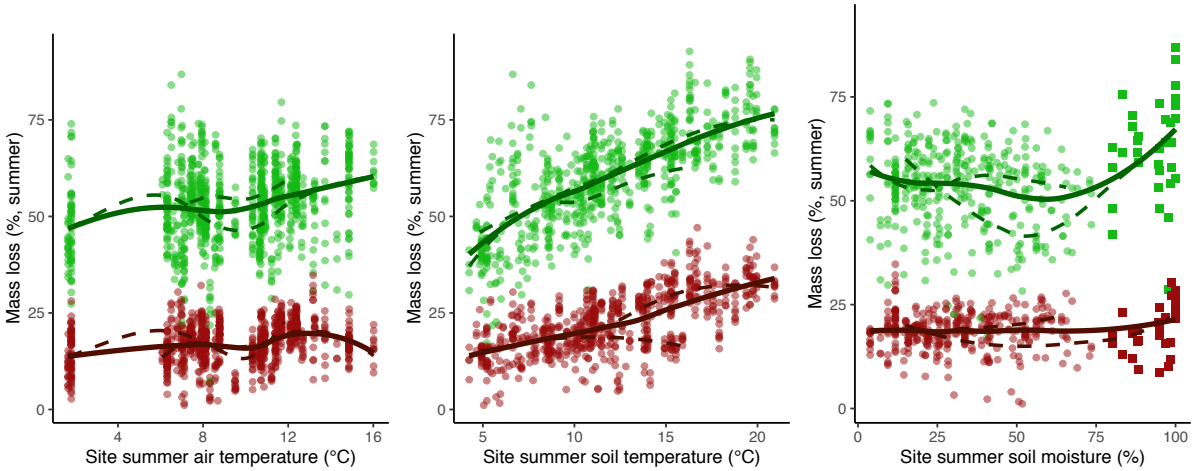

Figure S6. Overall, relationships between climate variables and mass loss were best described by linear rather than exponential models. In order to test the linearity of the relationships between climate variables and mass loss of tea types, we fit general additive models with a loess fit to the overall dataset (solid lines) and to the Western and Eastern hemispheres as two subsets of the data (dashed lines). The relationship between site summer soil moisture and green tea mass loss was more exponential, but this was driven by data from Svalbard located at particularly wet sites (square points) and thus we do not have confidence that the exponential relationships can be generalised to the tundra biome, which were better fit by hierarchical linear models (Fig. 3).

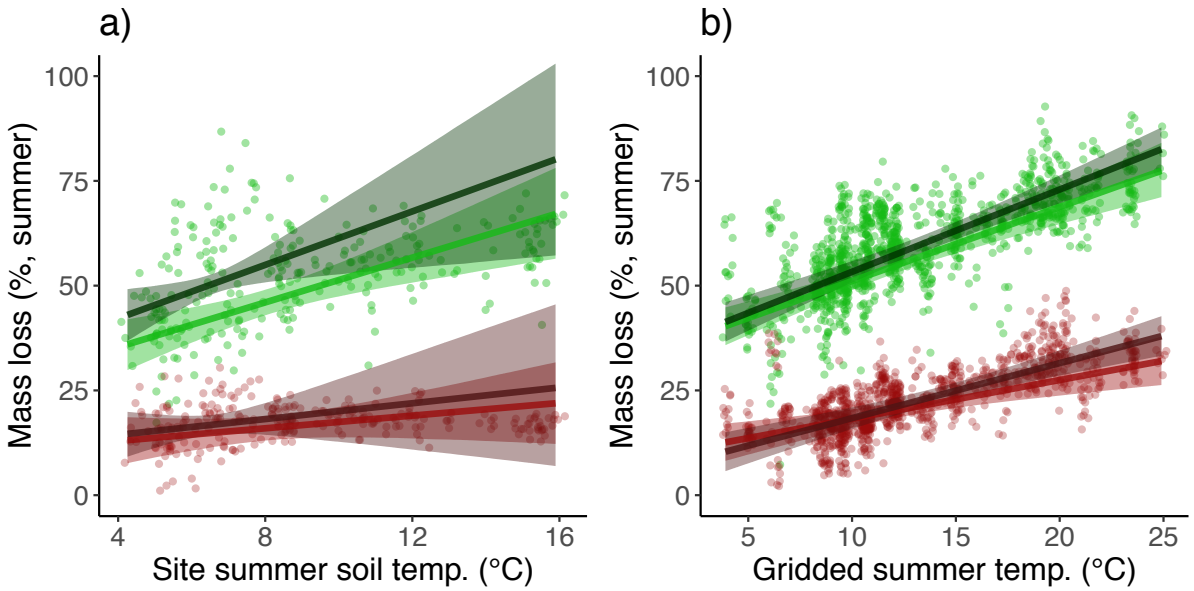

826
827

828 **Figure S7.** Soil moisture did not influence the relationships between soil temperature and
829 mass loss, but decomposition was higher at wetter versus drier sites at any given temperature.
830 Relationships between summer decomposition (mass loss), (a) measured soil temperature
831 and soil moisture, and (b) gridded temperature (CHELSA) and soil moisture (ESA). Models
832 incorporate the interaction between soil temperature and soil moisture. Lines indicate
833 predicted decomposition at upper (dark) and lower (light) quartiles of soil moisture,
834 representing wet and dry sites respectively, based on hierarchical Bayesian model fits with
835 97.5% credible intervals. Points indicate individual tea bag replicates. Colours indicate tea
836 type (red = rooibos tea, green = green tea). See Table S4 for model outputs.

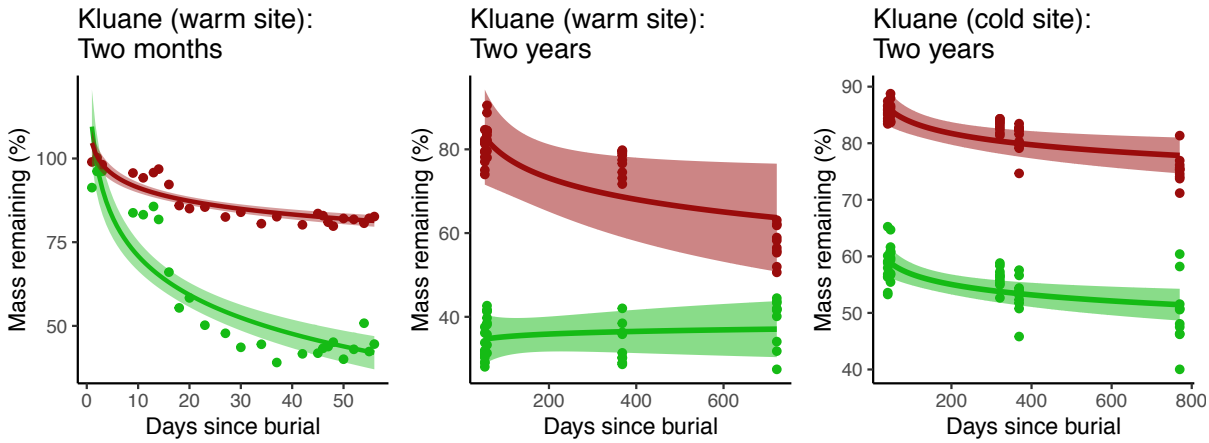

Figure S8. Mass loss of tea types did not converge after two years and stabilised after approximately 30 days. Mass remaining over time of rooibos and green tea at warm and cold tundra sites at the Kluane Lake location (see Table S1). Mass loss is calculated using a single-phase exponential decay decomposition model. (a) Mass remaining at the warm experimental site, with tea extracted every two days over a two-month summer period; (b) mass remaining at the warm experimental site with summer, one-year and two-year incubation lengths; and (c) mass remaining at the cold experimental site with summer, two-month, one-year and two-year incubation lengths.

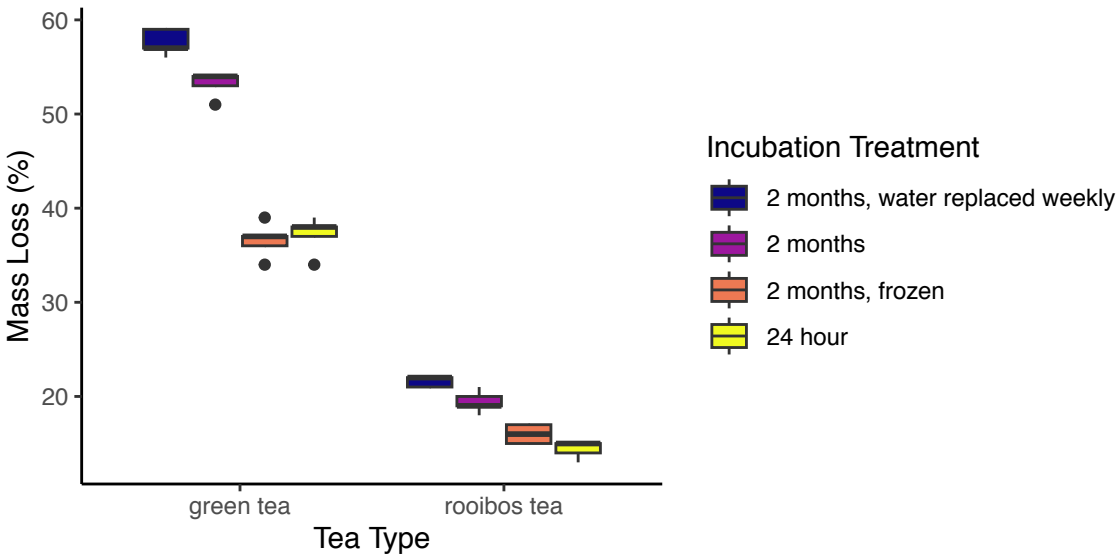

847
848

849 **Figure S9.** In order to test the influence of leaching, we conducted 2-month and 24-hour
850 incubations of green and rooibos tea in a laboratory environment at room temperature, in a
851 4°C fridge and a 20°C freezer. We found ~20% greater mass loss for green tea and ~7%
852 greater mass loss for rooibos tea in two-month incubations rather than in 24-hour incubations
853 in liquid water. Leaching was not strongly influenced by replacement of water and was slower
854 in frozen conditions for green and rooibos tea.

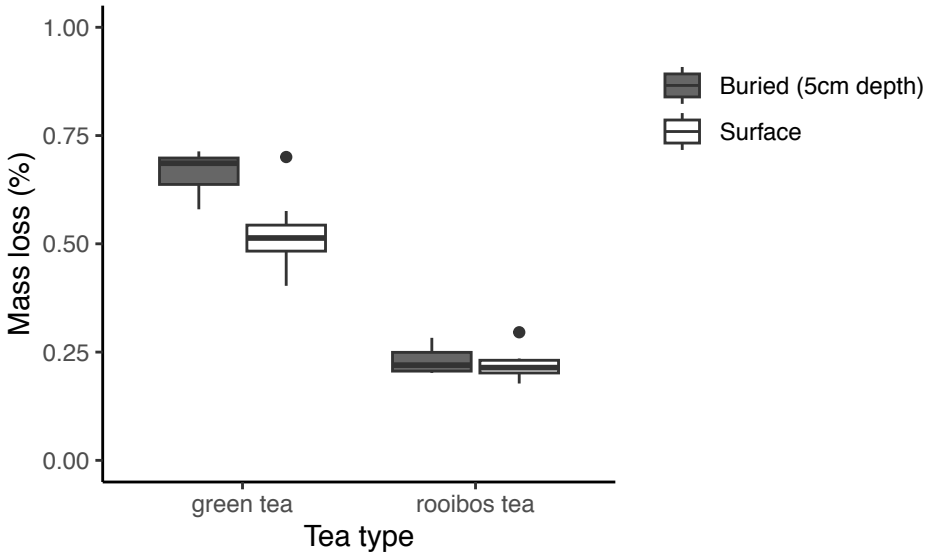

855
856

857 **Figure S10.** Mass loss of buried tea bags was significantly greater than tea placed on the
858 ground surface for green tea, but not different for rooibos tea. Teabags were incubated in a
859 common site (Kluane Lake, see Table S1) and were either buried at 5 cm depth directly in the
860 soil (grey) or placed within a litter bed and covered in a local litter medium (white), following
861 protocols outlined in Cornelissen et al. (2007). Teabags were incubated for one year, though
862 the time periods of incubation differed between the two treatment types (buried: June – June,
863 surface: August – August) as tea bags are taken from two different, but adjacent, experiments.
864 Stars indicate significance (***, $P < 0.001$, ns, $P > 0.05$, t-test).

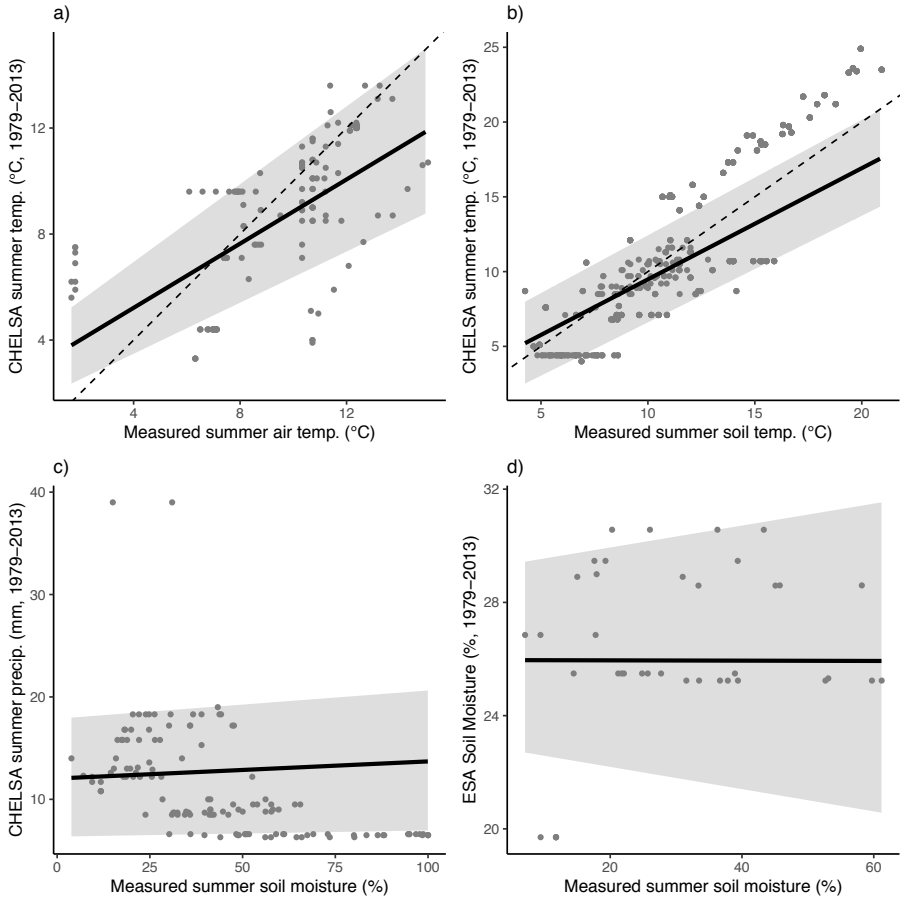

865
866

867 **Figure S11.** Site-measured environmental variables aligned with gridded climate variables for
868 summer temperature, but not summer soil moisture. Relationships between site-measured
869 environmental variables and gridded climate data for all tea bag sites with available data. Lines
870 indicate hierarchical Bayesian model fits and errors are 97.5% credible intervals. See Table
871 S5 for model outputs.

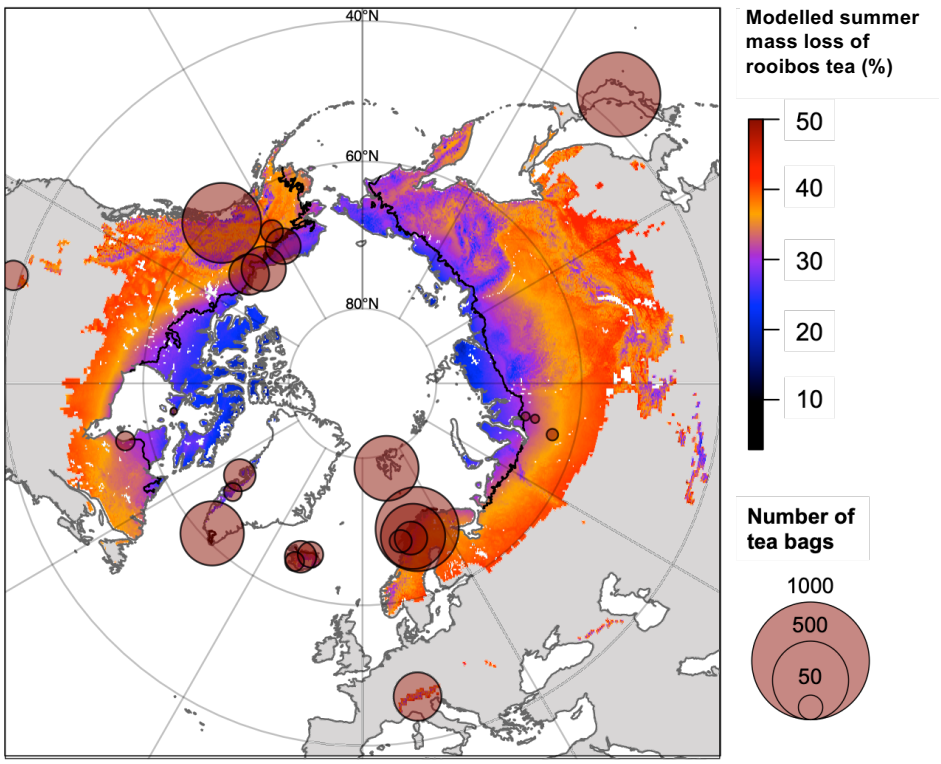

872
873

874 **Figure S12.** Modelled summer decomposition (percent mass loss) of rooibos tea for tundra
875 and sub-Arctic regions based on 1979 to 2013 mean summer air temperature (Climatologies
876 at high resolution for the Earth's land surface, CHELSA) and soil moisture (European Space
877 Agency data, ESA) from 1979 to 2013. Field collection locations are illustrated by red circles,
878 grouped by geographic region (Table S1, figure excludes Australian alpine region). Circle size
879 indicates the number of tea bag replicates within each geographic region. Tundra and sub-
880 Arctic classifications are based on Köppen-Geiger classification[42]. Ice-covered areas are
881 excluded. The circum-Arctic treeline is indicated with a black line[43].